Bismuth tellurides and sulphosalts from the Larga hydrothermal system, Metaliferi Mts., Romania: Paragenesis and genetic significance

N. J. Cook* and C. L. Ciobanu

Geological Survey of Norway, N-7491 Trondheim, Norway

ABSTRACT

Intermediate levels of the Larga-Faţa Băii field, Metaliferi Mts., Romania, are host to epithermal vein mineralization, small skarn-like bodies and 'geode'-like replacement ores, that together form a complex hydrothermal system rooted in the subjacent andesite stock. Silver-Pb-Bi sulphosalts, some with Sb and/or Se, are intimately associated with hessite and a range of Bi-tellurides with $Bi/(Te+S+Se) \leqslant 1$ (tetradymite, tellurobismuthite, tsumoite, Pb-free rucklidgeite) within all these ore types. Lillianite homologues, both ordered [4]L and [7]L derivatives (lillianite, gustavite), and disordered varieties are the most abundant sulphosalts, with subordinate bismuthinite derivatives (aikinite, krupkaite, bismuthinite). An exceptionally Ag-rich lillianite homologue, intimately intergrown with tetradymite and hessite, is identified as treasureite on the basis of chemical composition. Porphyry-style mineralization from 600 m beneath the studied level contains rucklidgeite as the single stable Bi-telluride. The trace mineralogy of the system is suggestive of a hydrothermal system strongly zoned with respect to f_{Te_2} and, to a lesser extent, also f_{S_2}. Mineralogical and textural evidence suggests that initial crystallization took place at temperatures in excess of 400ºC. The association of gold with Bi-minerals is linked to the role of Bi_{melt} as a scavenger for gold, and deposition within 'droplets' simultaneous with the formation of arsenopyrite from löllingite + pyrrhotite. Both Bi-tellurosulphides and sulphosalts are commonly non-stoichiometric, a fact that can be correlated with order-disorder in both series. When widely distributed, as in the Larga system, trace amounts of Bi-minerals (sulphosalts, tellurides/ tellurosulphides) have considerable, untapped potential as tracers of the physical-chemical character of an evolving hydrothermal system.

Keywords: tellurides, Bi-sulphosalts, compositional data, Larga, Metaliferi Mts., Romania.

Introduction

The Neogene gold deposits of the Metaliferi Mts., Romania (part of the South Apuseni Mountains, Fig. 1*a*), are considered classic examples of zoned, epithermal Cu-Zn-Pb-Au porphyry-vein systems (e.g. Ghiţulescu and Socolescu 1941; Ianovici *et al.*, 1969; Berbeleac, 1986; Alderton and Fallick, 2000). The region represents the type locality for a number of Te-bearing minerals

(native tellurium, tellurite, krennerite, nagyágite, petzite, sylvanite, muthmannite and stützite). The widespread distribution of Au- and Ag-tellurides is typical for the upper levels of many deposits, from which most historical production (from the Roman era to the 1940s) took place. Modern systematic microanalytical investigations of the mineralogy of the deposits or the hydrothermal systems in their totality are, however, relatively few, chiefly since the telluride-rich segments of many deposits (e.g. Săcărîmb, Bradişor, Musariu (Brad District) and Stănija) are entirely worked out. The occurrence and composition of tellurides has nevertheless been documented from several deposits, and in recent years, also confirmed by
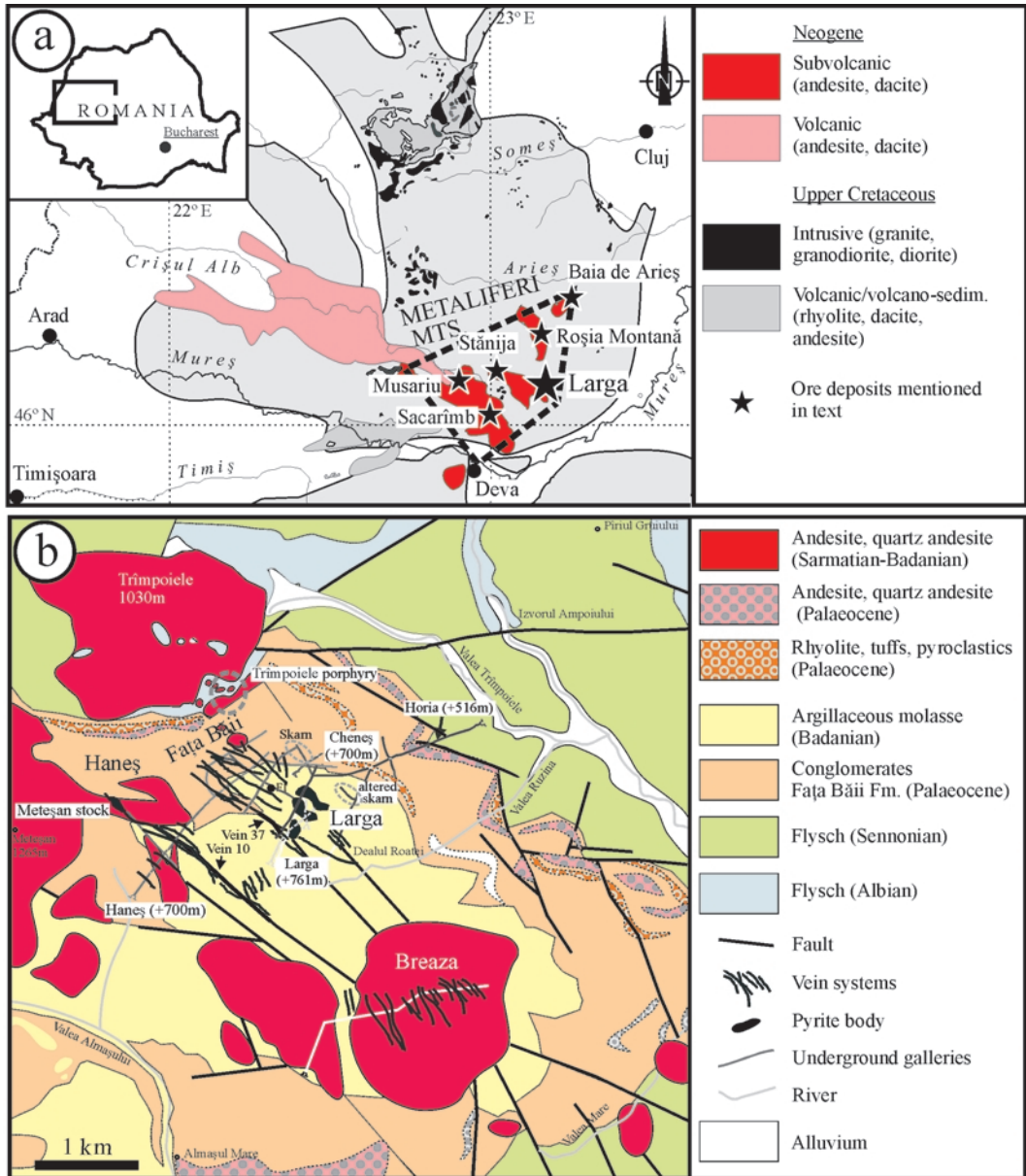
FIG. 1. (*a*) Geological sketch map of the Metaliferi Mts., showing the principal ore zones, including the Zlatna-Stănija volcanic zone that hosts the Faţa Băii-Haneş-Breaza-Larga-Trîmpoiele orefield. The dashed line shows the perimeter of the 'golden quadrangle'. (*b*) Geological-metallogenetic map of part of the Zlatna-Stănija volcanic zone, indicating the location of ores and underground galleries referred to in the text (projected to surface). Redrawn and modified after Borcoş *et al.* (1989).

microanalysis (e.g. Koch and Krasselly, 1950; Ramdohr and Udubaşa, 1973; Berbeleac and David, 1982; Popescu and Constantinescu, 1992; Popescu and Şimon, 1992; 1995; Cioflica *et al.*, 1993; Ioan *et al.*, 1993; Şimon *et al.*, 1994, 1995; Stanley *et al.*, 1994; Şimon and Alderton 1995*a,b*; Lupulescu (1997); Effenberger *et al.*, 1999; Shimizu *et al.*, 1999). Despite this, the occur-

rence, paragenetic position and genetic significance of tellurides and other trace minerals in deposits of the Metaliferi Mts. remains insufficiently understood, even though 'tetradymite' is sporadically reported as a trace mineral in the ores on the basis of optical identification (e.g. Ianovici *et al.*, 1969). There are no published accounts of bismuth sulphosalts as trace constituents in the ores, and even the widespread Sb-sulphosalt parageneses in several deposits in the region (e.g. Baia de Arieş; Cioflica *et al.*, 1999) are poorly constrained, due to lack of confirmation of optical mineral identification by microanalysis.

In this contribution, we focus on the occurrence of the abundant Bi-tellurides and sulphosalts within the zoned epithermal system from the Faţa Băii-Haneş-Breaza-Larga-Trîmpoiele district at the southeastern margin of the Metaliferi Mts. (Fig. 1a), their paragenetic relationships, and the genetic significance of these assemblages as indicators of ore formation conditions.

Geological setting

Larga, together with Faţa Băii, Haneş, Breaza and Trîmpoiele, constitutes a 10 km wide orefield (Fig. 1b) at the SE end of the Zlatna–Stănija volcanic alignment (Ghiţulescu and Socolescu 1941; Borcoş *et al.*, 1964, 1983). Calc-alkaline volcanic rocks of mid-Miocene age (main stage at ~13.5−12.5 Ma; see summary in Roşu, 2001) and associated volcanoclastics form a series of volcanic centres within Cretaceous flysch deposited onto a Jurassic ophiolitic basement. Both the ophiolite sequence and overlying flysch sediments have been emplaced tectonically as a nappe suite during Mid- and Late-Cretaceous events. Ores of the Zlatna area follow the style typical for the region, with initial porphyry copper roots, superimposed by polymetallic vein mineralization at higher levels (Borcoş, 1994; Berbeleac *et al.*, 1995). However, the Larga orefield itself has been modelled (Drew and Berger, 2001) in terms of a sudden vein opening above the porphyry root of the hydrothermal system. In parts, the vein systems are enriched in gold and or silver (1−5 g/t), but few reliable published grade data exist. Similarly, metal zonation patterns are not fully clear, although zinc and lead tend to increase with depth. There is also some evidence to show increasing Au with depth (e.g. Ianovici *et al.*, 1969, p. 645). The original Larga deposit, exploited from access gallery +761 m (Fig. 1b), was unique for the Metaliferi Mts., in that early

20th century exploitation concentrated on three lenses of high-grade gold-pyrite ore at the contact of Palaeocene Faţa Băii conglomerate and Badenian shale. More recently, including during the current (re-)exploration of the area (http://www.egoldfields.com), the 'Larga' deposit has come to mean a series of narrow quartz veins carrying Cu, Zn, Pb, Ag, and ~1−3 g/t Au that extend over a vertical extent of >500 m below the pyrite lenses. The largest of these, 'vein 37', has been partially exploited from the adjacent Haneş mine.

We have investigated mineralization in an area of ~1 km[2], accessible from the Horia exploration gallery (+516 m), 250 m below the exploited pyrite ores at Larga and the adjacent Faţa Băii and Haneş vein systems. Mineralization on the + 516 m level, thus represents an intermediate level in a strongly zoned epithermal system (Cu, Zn-Pb and Au, from bottom to top). Pyrite-arsenopyrite-gold vein mineralization found in the Horia gallery is positioned between the massive pyrite lenses at Larga *sensu stricto* and the Au-telluride-rich veins of the Faţa Băii deposit, some 250−300 m vertically above the Horia level, and the Trîmpoiele Cu-Au prospect, intersected by deep drilling at depths of 500−700 m beneath the Larga level.

Although the ores are variously Cu, Zn or Pb-rich, sometimes only consisting of pyrite, the diverse trace mineralogy and enrichment in tellurides is maintained throughout the entire 1.5 km vertical extent of the hydrothermal system. Elsewhere (Cook *et al.*, 2001; Cook and Ciobanu, 2002), we have documented the trend from Au-dominant telluride mineralogy (calaverite, sylvanite, with native tellurium and tellurite) at upper levels, to a dominance of Bi-tellurides and -tellurosulphides at depth.

On the Horia gallery (Fig. 2), we distinguish the following distinct types of mineralization: (1) a NW−SE, interrupted strike of veins across a horizontal distance of 800 m, hosted in Faţa Băii conglomerate. At the northwestern end (Cloşca gallery), directly underlying Faţa Băii, veins are Au-rich, pyrite-dominated, clustering around small andesite intrusions and include a 50 m diameter Cu-stockwork body. Abundant pyrrhotite relics and replacement of pyrrhotite by pyrite (± marcasite) at the hand-specimen scale, indicate pyrrhotite was the initial Fe-sulphide. At the southern termination of the Horia gallery, Vein 37 (at 625 m on 0 Vest gallery) is the longest (200 m) of several steeply dipping veins and lies
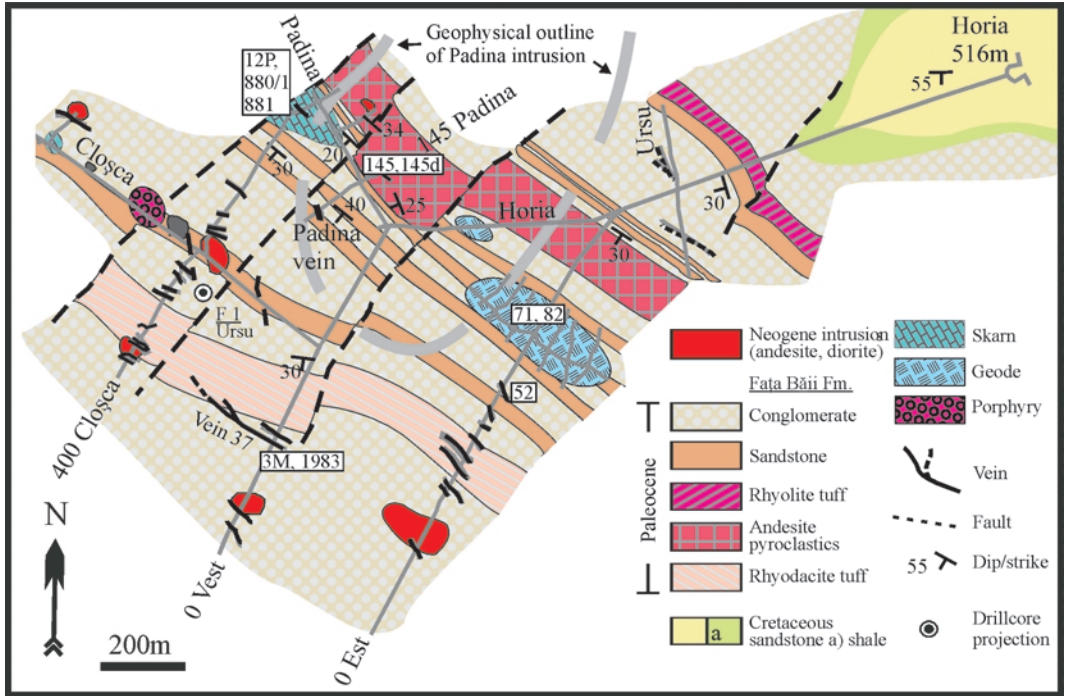
FIG. 2. Geological sketch map of the Horia Gallery and other underground workings accessed from the +516 m level (plan view). The detail is essentially based on mapping carried out by one of the present authors (CLC; Intreprinderea de Prospecţiuni Geologice şi Geofizice, Bucharest, unpubl. rep., 1991). The numbers in boxes are the locations of specific samples mentioned in the text and figures.

directly beneath the pyrite lenses (Figs 1 and 2). (2) A parallel strike of altered Zn-Pb skarn, some 400 m to northeast of the veins, relating to a limestone marker horizon in the conglomerate. These in turn can be sub-divided into a single lenticular body of mineralized boulders and 'geode'-style mineralization within advanced argillic alteration conglomerate, 500×150 m in dimensions on 0 Est gallery, and secondly, a body of garnet-epidote skarn hosting Zn-Pb-(Cu) mineralization (Padina gallery).

500 m further northwest, along the strike of the skarn, porphyry Cu-Au mineralization, as fine veinlets in altered andesite, is intersected in drillcore at the margin of the Trîmpoiele andesite at a depth of $950-1000$ m from surface. A second, smaller porphyry body is exposed on Cloşca gallery and has been followed down to 1000 m from surface (Ursu F-1 drillhole; Fig. 2). Our investigations show that the Te-rich character of the system clearly persists to this depth, but that Au-tellurides are absent in this porphyry mineralization.

Mineralogy

The mineral assemblage common to Vein 37, as seen in 0 Vest, and in the group of veins in 0 Est (Fig. 2) is arsenopyrite, pyrite, galena, sphalerite, chalcopyrite, marcasite, relict löllingite, pyrrhotite and gold ($Au_{90-96}Ag_{4-10}$). Particularly in 0 Est, a brecciated carbonate ($\pm$ quartz-clay mineral-chlorite) gangue hosts the sulphide ore. The As-rich character does not extend to the veins in Cloşca immediately subjacent to the Faţa Băii veins.

In the veins on 0 Vest and 0 Est galleries, gold occurs chiefly at grain boundaries within arsenopyrite containing löllingite relics (Fig. 3a). Arsenopyrite displays prominent compositional zonation, with Sb contents of up to 5 wt.%. In veins exposed on the + 516 m gallery, Bi-tellurides/tellurosulphides are associated with hessite and galena (Fig. 3b and c). These are typical as composite inclusions in arsenopyrite, pyrite, sphalerite and more rarely galena, and an association with gold is common. They are
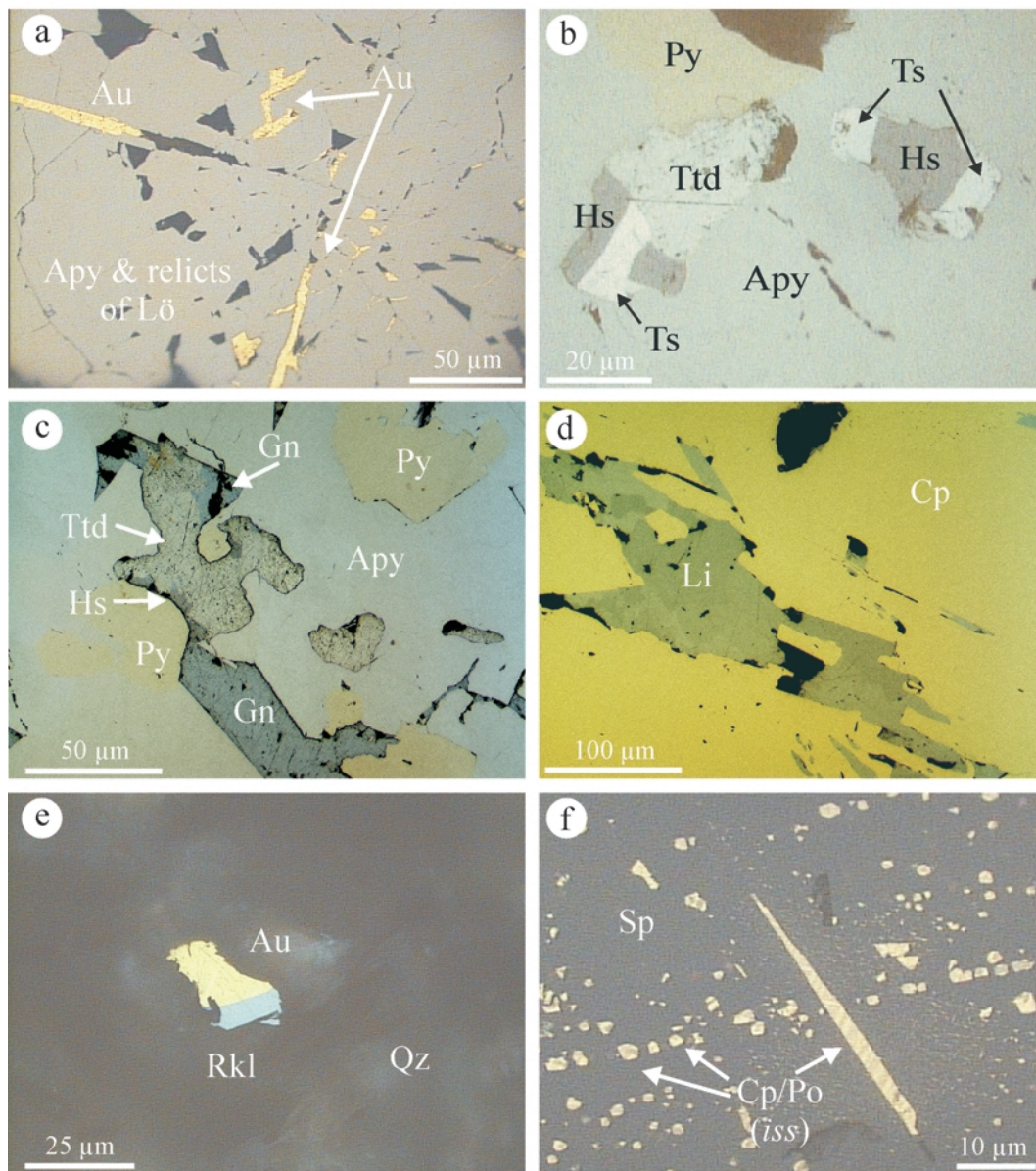
FIG. 3. Photomicrographs in reflected light showing paragenetic relationships of ore minerals in Larga ores. (*a*) Inclusions of gold (Au) within an intergrowth of arsenopyrite (Apy) and relict löllingite (Lo). Sample: 52 (0 Est gallery). (*b*) Association of tellurides in pyrite (Py) and arsenopyrite (Apy) within typical vein mineralization. Ttd: tetradymite, Hs: hessite, Ts: tsumoite. Sample: 3M (Vein 37 at 625 m, 0 Vest gallery). (*c*) Inclusions of tetradymite (Ttd) within a matrix of arsenopyrite (Apy) and pyrite (Py). Note the co-existence of hessite (Hs) and galena (Gn). Sample: 3M (Vein 37 at 625 m, 0 Vest gallery). (*d*) Typical occurrence of bismuth sulphosalts, in this case dominantly composed of Sb-bearing lillianite (Li) as inclusions in chalcopyrite (Cp). Sample: 145 (vein in Padina gallery). (*e*) Association of gold (Au) and rucklidgeite (Rkl) in quartz within the Trîmpoiele porphyry deposit. Sample: T960. (*f*) Inclusions of chalcopyrite and pyrrhotite crystallized from intermediate solid solution (Cp/Po) within Haneş veins dominated by sphalerite (Sp). Sample: 1963.

markedly less common in the Cloşca veins, which instead contain Pb-Sb sulphosalts. Bismuth sulphosalts occur sporadically within the veins, in some cases, particularly within the Padina vein, becoming a major component (>1 vol.%) of the galena-pyrite ores (Fig. 3d). Cervelleite, $(Ag,Cu)_4TeS$, is a minor accessory; its association with hessite, galena and arsenopyrite, and its chemistry have been described elsewhere (Cook and Ciobanu, 2003). Other trace minerals include secondary acanthite and two members of the canfieldite-argyrodite series, Ag_8SnS_6 and $(Ag_{7.39}Cu_{0.73}Fe_{0.29})_{8.41}Ge_{0.77}S_{5.82}$.

The skarn ore comprises sphalerite (8−9 wt.% Fe), seleniferous galena (up to 7.3 wt.% Se), pyrite, arsenopyrite, with accessory stannite and zoned tetrahedrite-tennantite with typical compositions in the range $Cu_{10}(Fe_{0.2−0.3}Zn_{1.7−1.8})_2 (As_{1.6−2.5}Sb_{1.5−2.4})_4S_{13}$. Bismuth tellurides and tellurosulphides occur at sphalerite- and pyrite-gangue boundaries or enclosed within sphalerite. Assemblages are tellurobismuthite + tetradymite; more rarely tellurobismuthite + Pb-free rucklidgeite, with µm-scale inclusions of galena abundant in tellurobismuthite. The pyrrhotite is largely replaced by pyrite and/or marcasite. In both styles of mineralization, hessite and altaite are persistent accessories. Sylvanite and petzite-gold-hessite decomposition products of sylvanite are both identified in minor quantities.

The aforementioned porphyry style mineralization in Trîmpoiele is dominated by quartz veinlets within altered andesite and biotite hornfels, and carry sporadic pyrrhotite (both hexagonal and monoclinic), chalcopyrite, seleniferous galena and molybdenite; pyrite is abundant in the upper half of the stock. Gold is abundant within the sections we have investigated, as is a close association with the sole Bi-telluride, rucklidgeite (Fig. 3e). Accessories include altaite, clausthalite and bismuthinite.

We have also examined veins in the Haneş mine from a level ~100 m lower than the Horia gallery. These veins are sphalerite-dominant, with accessory stannite. Within µm-scale inclusions in sphalerite and pyrite, there is abundant evidence for initial intermediate solid solution (*iss*), from which chalcopyrite and pyrrhotite exsolved (Fig. 3f).

Microanalysis

EPMA was carried out using the JEOL JXA 8600 instruments at Bristol University and the Natural History Museum, London (both UK). Operating conditions were 20 nA/15 kV in both cases. Standards and radiations used were as follows: Bi_2S_3 (Bi-$M\alpha$), PbS (Pb-$L\alpha$/$M\alpha$, S-$K\alpha$), FeS_2 (Fe-$K\alpha$, S-$K\alpha$), $CuFeS_2$ (Cu-$K\alpha$), ZnS (Zn-$K\alpha$), Bi_2Te_3 (Te-$L\alpha$), Bi_2Se_3 (Se-$L\alpha$), Ag metal ($L\alpha$), CdS (Cd-$L\alpha$) and Sb_2S_3 (Sb-$L\alpha$). Overlap and matrix corrections were carried out following established practices and software in the two laboratories. We have analysed the same and similar material from Larga in other laboratories. e.g. Adelaide, Australia and Salzburg, Austria[1], at a variety of operating conditions, and are satisfied that the data set is not affected by systematic errors beyond normal instrumental precision.

Bi-tellurides/tellurosulphides

Mineralogy

In Vein 37 (0 Vest gallery), tetradymite and tsumoite are abundant as 20−100 µm inclusions in arsenopyrite, associated with galena and hessite. The morphology of the composite inclusions (Fig. 4a) indicates crystallization from a melt under equilibrium conditions. Minor quantities of Bi_3Te_4, a virtually Pb-free rucklidgeite, are noted at the boundaries of tetradymite. Although Au-tellurides are scarce in veins from the intermediate levels, they are nevertheless present as sylvanite (and breakdown products thereof), native tellurium, tellurobismuthite and hessite (Fig. 4b). The skarn ores contain the persistent assemblage tetradymite + tellurobismuthite + altaite, within calcite gangue, forming a rim on pyrite, or enclosed in galena, and rarely pyrite (Fig. 4c−f). Both tetradymite (Fig. 4e) and tellurobismuthite persistently contain sub-5 µm inclusions of galena, and more rarely, altaite. Pb-bearing rucklidgeite, $(PbBi)_3Te_4$, is the sole Bi-telluride observed in the Trîmpoiele porphyry. The 'geode' ores contain abundant tellurides as inclusions in sphalerite and pyrite (Fig. 5a). These are typically composite and consist of hessite, tetradymite, altaite and volynskite (Fig. 5b and c), but also contain relatively large amounts of a conspicuous intergrowth of decomposition products of a Au-Ag-Te-S phase (Fig. 5d).

---

[1] The analyses of a pavonite homologue (Table 3) were obtained in Salzburg: JEOL JXL-8600; 25 kV, 35 na, S $K\alpha$ (Bi_2S_3), Ag $L\alpha$ (Ag), Sb $L\alpha$ (Sb_2S_3), Cd $L\alpha$ (CdTe), Te $L\alpha$ (CdTe), Se $K\alpha$ (Bi_2Se_3), Bi $L\alpha$ (Bi_2S_3), Pb $L\alpha$ (PbS), Cu $K\alpha$ ($CuFeS_2$).
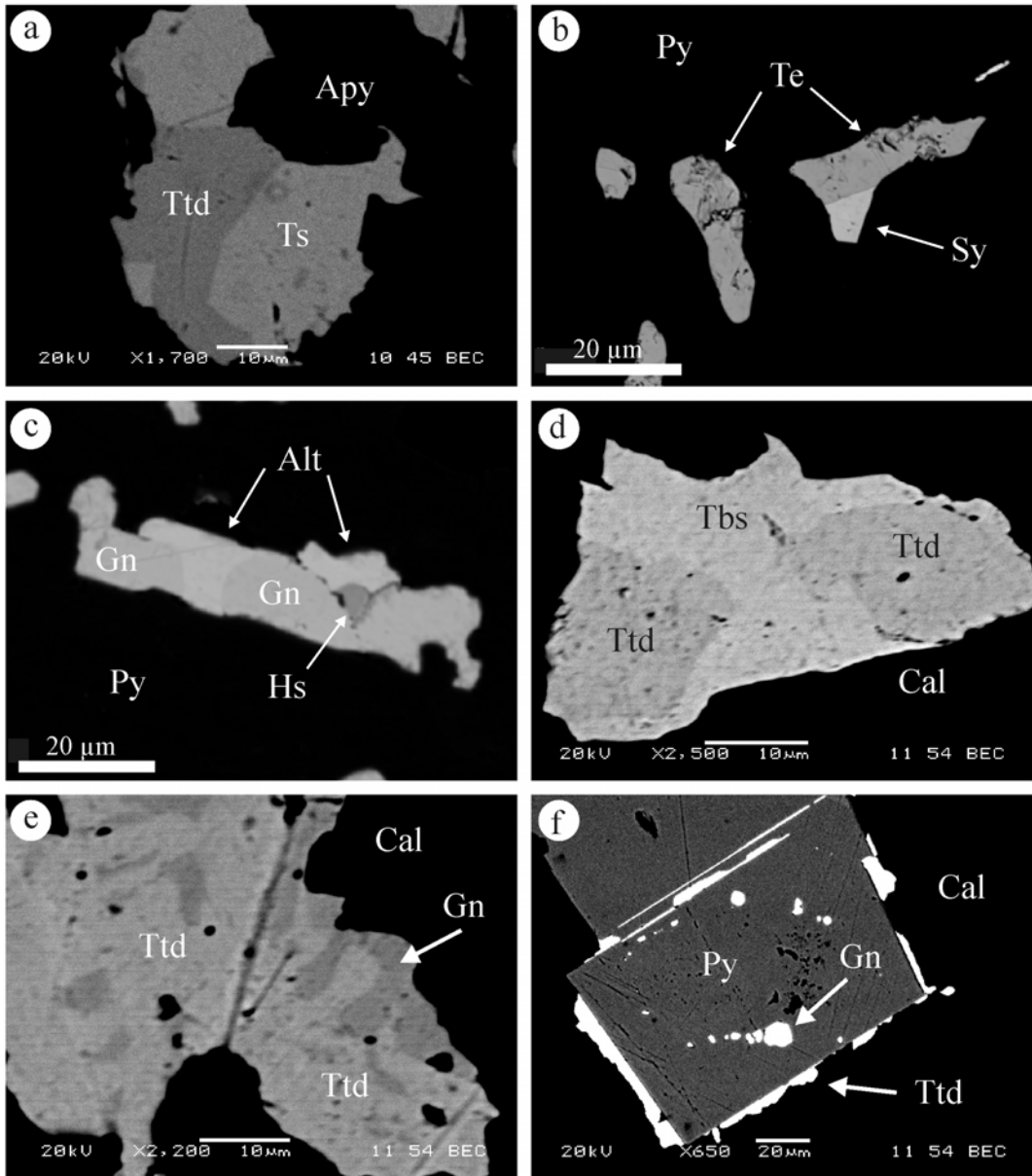
FIG. 4. BSE images showing the habit and association of Bi-tellurides in Larga ores. (*a*) Association of tetradymite (Ttd) and tsumoite (Ts) as inclusions within arsenopyrite (Apy) in vein ores. Note curvilinear equilibrium boundary between the two Bi-minerals. Sample: 3M (Vein 37 at 625 m, 0 Vest gallery). (*b*) Association of sylvanite (Sy), native tellurium (Te) and tellurobismuthite (Tbs) within pyrite (Py). Sample: 3M (Vein 37 at 625 m, 0 Vest gallery). (*c*) Assemblage containing coexisting altaite (Alt) and galena (Gn), with minor hessite (Hs). Sample: 881 (skarn, Padina gallery). (*d*) Equilibrium association of tetradymite (Ttd) and tellurobismuthite (Tbs) in calcite (Cal) from skarn ores. Sample: 12P (skarn, Padina gallery). (*e*) Larger grain of tetradymite (Ttd) within calcite from skarn ores, containing exsolved galena (Gn). Sample: 12P (skarn, Padina gallery). (*f*) Narrow rim of tetradymite (Ttd) surrounding pyrite (Py) in calcite (Cal) from skarn ores. Gn: galena. Sample: 12P (skarn, Padina gallery).

Composition

Compositional data for tetradymite and tsumoite from the veins are summarized in Table 1 and plotted on Fig. 6. All tetradymite analyses display the same slight enrichment of (S+Se) relative to Te that is seen in almost all published analyses for the mineral (Cook *et al.*, in review). Analysed tetradymite compositions contain up to 0.3 atoms per formula unit (a.p.f.u.) Se, and plot along the tetradymite-kawazulite join (Fig. 6*b*). Some tetradymite contains several wt.% Pb, attributable to sub-µm inclusions of galena. Co-existing tsumoite typically has a Bi/Te ratio of ~0.90−0.97, consistent with the divergence from stoichiometry commonly seen in this mineral (e.g. Bayliss,

1991). Tetradymite from the skarn mineralization shows a similar distribution (Fig. 6) as in the vein ores, whereas the co-existing tellurobismuthite is effectively stoichiometric Bi_2Te_3. Rucklidgeite from the Trîmpoiele porphyry body contains Pb, with limited variation in composition between $(Pb_{0.82-0.87}Bi_{2.11-2.16})_3(Te,Se,S)_4$, and no Ag present (cf. Kase *et al.*, 1993). Conspicuous, however, is the presence of (Se+S) in all analyses, between 0.1 and 0.3 a.p.f.u. (Table 1).

Bismuth sulphosalts

Mineralogy

Bi-sulphosalts are rare but persistent accessories of both vein and skarn ores exposed on the Horia
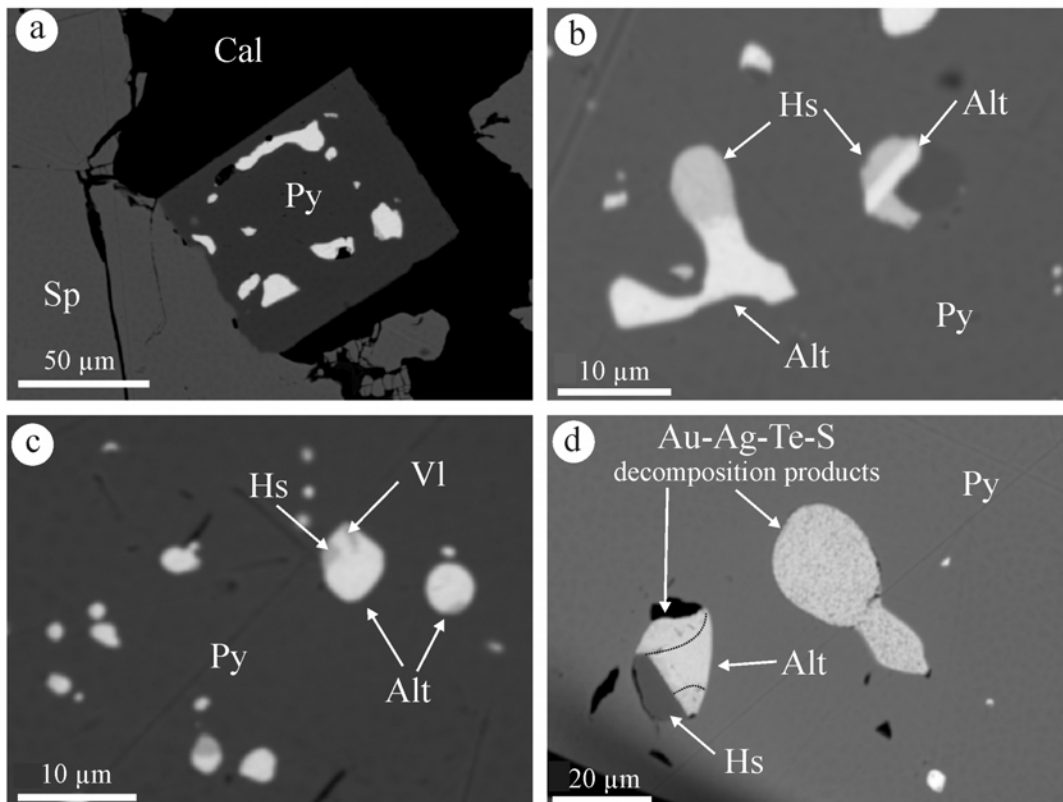

FIG. 5. BSE images showing the habit and association of Bi-tellurides in 'geode' type ores; all from sample: 71 (0 Est gallery). (*a*) Included blebs of tellurides (bright white) within pyrite (Py). Sp: sphalerite; Cal: calcite. (*b*) Composite inclusions of hessite (Hs) and altaite (Alt) within pyrite (Py). (*c*) Similar bleb-like telluride inclusions within pyrite (Py), consisting of hessite (Hs), altaite (Alt) and volynskite (Vl). (*d*) Composite, bleb-like inclusions in pyrite (Py), consisting of hessite (Hs), altaite (Alt) and a decomposition intergrowth with a bulk composition approximating to $Ag_3Au(S,Te)_2$. Note curvilinear equilibrium boundaries.

TABLE 1. Electron microprobe analyses of Bi-tellurides and tellurosulphides.

Tetradymite	Cu	Ag	Fe	Cd	Pb	Bi	Sb	S	Se	Te	Total	Calculated formula (on the basis of 5 a.p.f.u.)*
1983/1 (vein) a7.p1 B56	<mdl	0.16	0.13	<mdl	<mdl	59.26	0.82	4.64	0.47	33.34	98.82	$(Bi_{2.02}Sb_{0.05})_{2.07}(Te_{1.86}Se_{0.04}S_{1.03})_{2.93}$
a10.p (§)	<mdl	0.20	0.29	<mdl	<mdl	58.79	0.39	4.66	0.51	34.81	99.65	$(Bi_{1.99}Sb_{0.02})_{2.01}(Te_{1.92}Se_{0.05}S_{1.02})_{2.99}$
3M (vein) a1.gr2	0.06	0.17	0.12	<mdl	<mdl	59.40	0.23	4.14	1.12	34.68	99.90	$(Bi_{2.03}Sb_{0.01})_{2.04}(Te_{1.94}Se_{0.10}S_{0.92})_{2.96}$
a8.gr19	<mdl	0.27	0.25	<mdl	<mdl	58.47	0.16	4.03	1.49	34.07	98.74	$(Bi_{2.03}Sb_{0.01})_{2.03}(Te_{1.93}Se_{0.14}S_{0.90})_{2.97}$
a1.gr2	<mdl	0.22	0.17	0.08	<mdl	58.74	0.21	3.87	1.83	34.23	99.35	$(Bi_{2.04}Sb_{0.01})_{2.05}(Te_{1.91}Se_{0.18}S_{0.86})_{2.95}$
a7.gr18	<mdl	0.14	0.17	<mdl	<mdl	59.59	0.12	3.88	1.96	34.26	100.11	$(Bi_{2.02}Sb_{0.01})_{2.03}(Te_{1.93}Se_{0.17}S_{0.87})_{2.97}$
a3.gr15	<mdl	0.25	0.22	0.07	<mdl	59.54	0.19	3.69	2.25	34.10	100.30	$(Bi_{2.05}Sb_{0.01})_{2.06}(Te_{1.91}Se_{0.20}S_{0.83})_{2.94}$
a2.gr7	0.06	0.17	0.21	<mdl	<mdl	58.78	0.11	3.53	2.71	33.97	99.54	$(Bi_{2.04}Sb_{0.02})_{2.06}(Te_{1.89}Se_{0.25}S_{0.80})_{2.94}$
a3.gr16	0.18	0.38	0.31	<mdl	<mdl	59.48	0.25	3.57	2.79	33.66	100.61	$(Bi_{2.03}Sb_{0.01})_{2.04}(Te_{1.92}Se_{0.25}S_{0.79})_{2.94}$
a3.gr13	0.16	0.19	0.57	<mdl	<mdl	58.63	0.14	3.39	2.91	33.68	99.68	$(Bi_{2.04}Sb_{0.01})_{2.05}(Te_{1.91}Se_{0.27}S_{0.77})_{2.95}$
a2.gr11	0.12	<mdl	0.98	<mdl	<mdl	58.45	0.23	3.01	3.80	33.36	99.94	$(Bi_{2.05}Sb_{0.01})_{2.06}(Te_{1.91}Se_{0.35}S_{0.68})_{2.95}$
a2.gr11	<mdl	0.15	0.61	<mdl	0.15	58.45	0.26	3.02	4.07	33.23	99.95	$(Pb_{0.01}Bi_{2.03}Sb_{0.02})_{2.06}(Te_{1.89}Se_{0.37}S_{0.68})_{2.94}$
Mean (*n* = 39)	**0.04**	**0.19**	**0.45**	**0.03**	**0.08**	**58.87**	**0.18**	**3.58**	**2.44**	**33.91**	**99.77**	**$(Bi_{2.04}Sb_{0.01})_{2.05}(Te_{1.93}Se_{0.22}S_{0.80})_{2.96}$**
st. dev.			0.27			0.73	0.06	0.42	0.74	0.33	0.58	
12P (skarn) a2.gr2	0.08	0.11	0.05	0.06	1.23	58.30	0.06	4.16	1.15	34.88	100.08	$(Pb_{0.04}Bi_{1.99})_{2.03}(Te_{1.95}Se_{0.10}S_{0.92})_{2.97}$
a2.gr2	0.17	0.01	0.05	0.06	0.28	58.17	0.07	4.02	1.26	34.96	99.03	$(Pb_{0.01}Bi_{2.00})_{2.01}(Te_{1.97}Se_{0.11}S_{0.90})_{2.99}$
a2.gr3	0.09	0.08	0.07	<mdl	0.73	57.99	<mdl	4.12	1.37	34.79	99.24	$(Pb_{0.03}Bi_{1.98})_{2.01}(Te_{1.95}Se_{0.12}S_{0.92})_{2.99}$
a3.gr1	0.13	<mdl	0.05	<mdl	0.00	58.41	<mdl	4.04	1.09	35.11	98.82	$Bi_{2.01}(Te_{1.98}Se_{0.10}S_{0.90})_{2.99}$
a3.gr2	0.12	<mdl	<mdl	<mdl	0.52	58.30	<mdl	4.30	0.51	35.05	98.79	$(Pb_{0.02}Bi_{2.00})_{2.02}(Te_{1.97}Se_{0.05}S_{0.96})_{2.98}$
a3.gr3	0.25	<mdl	0.00	0.07	0.21	59.16	<mdl	3.73	1.54	34.86	99.83	$(Pb_{0.01}Bi_{2.04})_{2.05}(Te_{1.97}Se_{0.14}S_{0.84})_{2.95}$
Mean (*n* = 10)	**0.15**	**0.03**	**0.03**	**0.04**	**0.77**	**58.19**	**0.05**	**4.06**	**1.14**	**34.91**	**99.37**	**$(Pb_{0.03}Bi_{2.00})_{2.03}(Te_{1.96}Se_{0.10}S_{0.91})_{2.97}$**
St. dev.		0.10			0.71	0.43			0.20	0.29	0.46	0.60	
Tsumoite												**(on the basis of 2 atoms p.f.u.)***
3M (vein) a2.gr7	0.06	<mdl	0.46	0.07	0.04	58.18	0.06	<mdl	0.74	39.70	99.30	$Bi_{0.93}(Te_{1.04}Se_{0.03})_{1.07}$
a2.gr6	0.11	<mdl	0.49	0.11	0.59	62.32	0.18	<mdl	0.86	35.13	99.77	$(Pb_{0.01}Bi_{1.01})_{1.02}(Te_{0.93}Se_{0.04})_{0.97}$
a2.gr6	0.08	0.21	0.50	<mdl	1.62	62.95	0.10	<mdl	0.77	35.63	100.69	$(Pb_{0.01}Bi_{1.02})_{1.03}(Te_{0.94}Se_{0.03})_{0.97}$
a2.gr11	0.11	0.09	0.87	<mdl	0.82	60.98	0.11	<mdl	1.03	35.74	99.75	$(Pb_{0.01}Bi_{1.01})_{1.00}(Te_{0.95}Se_{0.04})_{0.99}$
a3.gr15	<mdl	0.10	0.25	<mdl	0.56	59.27	0.08	<mdl	0.69	37.93	98.87	$(Pb_{0.01}Bi_{0.96})_{0.97}(Te_{1.00}Se_{0.03})_{1.03}$
a3.gr15	<mdl	0.08	0.26	0.06	0.72	58.99	0.07	<mdl	0.70	38.07	98.95	$(Pb_{0.01}Bi_{0.95})_{0.96}(Te_{1.01}Se_{0.03})_{1.04}$
a3.gr15	<mdl	<mdl	0.28	<mdl	0.65	59.62	<mdl	<mdl	0.67	37.92	99.13	$(Pb_{0.01}Bi_{0.96})_{0.97}(Te_{1.00}Se_{0.03})_{1.03}$
Mean (*n* = 20)	**0.05**	**0.11**	**0.58**	**0.05**	**0.54**	**59.89**	**0.08**	**0.07**	**0.77**	**37.45**	**99.59**	**$(Pb_{0.01}Bi_{0.97})_{0.98}(Te_{0.99}Se_{0.03})_{1.02}$**
St. dev.			0.38			0.26	1.67			0.16	1.51	0.71	
Tellurobismuthite												**(on the basis of 5 atoms p.f.u.)***
12P (skarn) a1.gr1	0.15	<mdl	<mdl	<mdl	<mdl	52.40	0.24	<mdl	0.37	46.32	99.48	$(Bi_{2.01}Sb_{0.02})_{2.03}(Te_{2.92}Se_{0.04}S_{0.01})_{2.97}$
a1.gr3	0.10	<mdl	<mdl	<mdl	<mdl	52.58	<mdl	<mdl	0.35	46.83	99.85	$Bi_{2.02}(Te_{2.94}Se_{0.04}S_{0.01})_{2.98}$
a2.gr1	<mdl	<mdl	<mdl	0.08	<mdl	52.08	0.22	0.06	0.38	46.55	99.37	$(Bi_{2.00}Sb_{0.01})_{2.01}(Te_{2.93}Se_{0.04}S_{0.02})_{2.99}$
a3.gr1	0.09	0.09	<mdl	<mdl	<mdl	51.63	0.15	0.06	0.42	47.02	99.45	$(Bi_{1.98}Sb_{0.01})_{1.99}(Te_{2.95}Se_{0.04}S_{0.02})_{3.01}$
a3.gr3	0.23	0.08	0.06	<mdl	<mdl	51.64	0.04	0.07	0.46	46.34	98.91	$Bi_{2.00}(Te_{2.93}Se_{0.05}S_{0.02})_{3.00}$
Mean (*n* = 11)	**0.16**	**0.04**	**0.03**	**0.04**		**51.72**	**0.15**	**0.05**	**0.36**	**46.49**	**99.31**	**$(Bi_{2.00}Sb_{0.01})_{2.01}(Te_{2.94}Se_{0.04}S_{0.01})_{2.99}$**
st. dev.						0.70			0.05	0.34	0.54	
Low-Pb-rucklidgeite												**(on the basis of 7 atoms p.f.u.)***
3M (vein) a1.p3	<mdl	<mdl	0.69	<mdl	0.76	52.64	0.17	<mdl	0.22	44.80	99.28	$(Pb_{0.04}Bi_{2.89}Sb_{0.02})_{2.95}(Te_{4.02}Se_{0.03})_{4.05}$
a12.p2	<mdl	0.16	0.34	<mdl	<mdl	52.93	0.23	0.12	0.43	44.94	99.16	$(Bi_{2.87}Sb_{0.04})_{2.91}(Te_{3.99}Se_{0.06}S_{0.04})_{4.09}$
a22.p1	0.11	<mdl	0.50	<mdl	<mdl	52.64	0.39	0.16	0.35	43.59	97.74	$(Bi_{2.91}Sb_{0.04})_{2.95}(Te_{3.94}Se_{0.05}S_{0.06})_{4.05}$
a22.p2	<mdl	<mdl	0.45	<mdl	0.97	52.53	<mdl	<mdl	0.40	44.63	98.98	$(Pb_{0.05}Bi_{2.88})_{2.93}(Te_{4.01}Se_{0.06})_{4.06}$
a22.p3	0.14	0.11	0.48	<mdl	<mdl	52.85	0.37	0.09	0.45	44.43	98.92	$(Bi_{2.89}Sb_{0.03})_{2.92}(Te_{3.98}Se_{0.07}S_{0.03})_{4.07}$
a22.p8	<mdl	<mdl	0.56	<mdl	<mdl	52.97	0.19	<mdl	0.39	44.29	98.40	$(Bi_{2.92}Sb_{0.02})_{2.94}(Te_{4.00}Se_{0.06})_{4.06}$
a23.p2	0.13	<mdl	0.94	<mdl	0.95	52.64	0.00	<mdl	0.38	43.34	98.38	$(Pb_{0.05}Bi_{2.93})_{2.98}(Te_{3.96}Se_{0.06})_{4.02}$
a23.p3	<mdl	<mdl	1.00	<mdl	<mdl	52.78	0.48	0.22	0.49	43.55	98.52	$(Bi_{2.89}Sb_{0.05})_{2.94}(Te_{3.91}Se_{0.07}S_{0.08})_{4.06}$
a23.p4	<mdl	<mdl	0.85	<mdl	0.58	52.74	0.34	<mdl	0.41	44.10	99.02	$(Pb_{0.03}Bi_{2.90})_{2.96}(Te_{3.98}Se_{0.06})_{4.04}$
Mean (*n* = 15)	**0.05**	**0.03**	**0.71**		**0.34**	**52.44**	**0.29**	**0.09**	**0.38**	**44.14**	**98.48**	**$(Pb_{0.02}Bi_{2.88}Sb_{0.03})_{2.93}(Te_{3.98}Se_{0.06}S_{0.03})_{4.07}$**
St. dev.			0.31			0.80			0.12	0.79	0.68	
Pb-rucklidgeite												
T960 a1.,gr1	<mdl	<mdl	<mdl	0.09	15.74	39.91	0.12	0.15	0.97	43.01	100.00	$(Pb_{0.86}Bi_{2.15}Sb_{0.01})_{3.02}(Te_{3.79}Se_{0.14}S_{0.05})_{3.98}$
(porphyry) a1.,gr1	<mdl	<mdl	<mdl	0.11	15.48	40.28	0.08	0.19	0.84	43.22	100.20	$(Pb_{0.84}Bi_{2.16}Sb_{0.01})_{3.01}(Te_{3.80}Se_{0.12}S_{0.07})_{3.99}$
a1.gr1	<mdl	<mdl	<mdl	0.08	15.45	40.37	0.16	0.15	0.88	43.14	100.23	$(Pb_{0.84}Bi_{2.17}Sb_{0.01})_{3.02}(Te_{3.80}Se_{0.13}S_{0.05})_{3.98}$
a2.gr1	<mdl	<mdl	<mdl	<mdl	15.62	39.39	0.16	0.15	1.23	42.46	99.00	$(Pb_{0.85}Bi_{2.14}Sb_{0.01})_{3.00}(Te_{3.77}Se_{0.18}S_{0.05})_{4.00}$
a3.gr1	<mdl	<mdl	<mdl	0.10	15.38	38.66	0.11	0.15	0.93	42.83	98.17	$(Pb_{0.85}Bi_{2.12}Sb_{0.01})_{2.98}(Te_{3.84}Se_{0.13}S_{0.05})_{4.02}$
a5.gr1	<mdl	<mdl	<mdl	<mdl	15.35	39.90	0.00	0.45	1.29	42.82	99.80	$(Pb_{0.82}Bi_{2.12})_{2.94}(Te_{3.73}Se_{0.18}S_{0.15})_{4.06}$
Mean (*n* = 11)				**0.05**	**15.34**	**39.38**	**0.11**	**0.21**	**1.15**	**42.50**	**98.75**	**$(Pb_{0.84}Bi_{2.14}Sb_{0.01})_{2.99}(Te_{3.78}Se_{0.16}S_{0.07})_{4.01}$**
St. dev.					0.33	0.66	0.04	0.14	0.26	0.56	1.21	

all analyses made at NHM (except §)
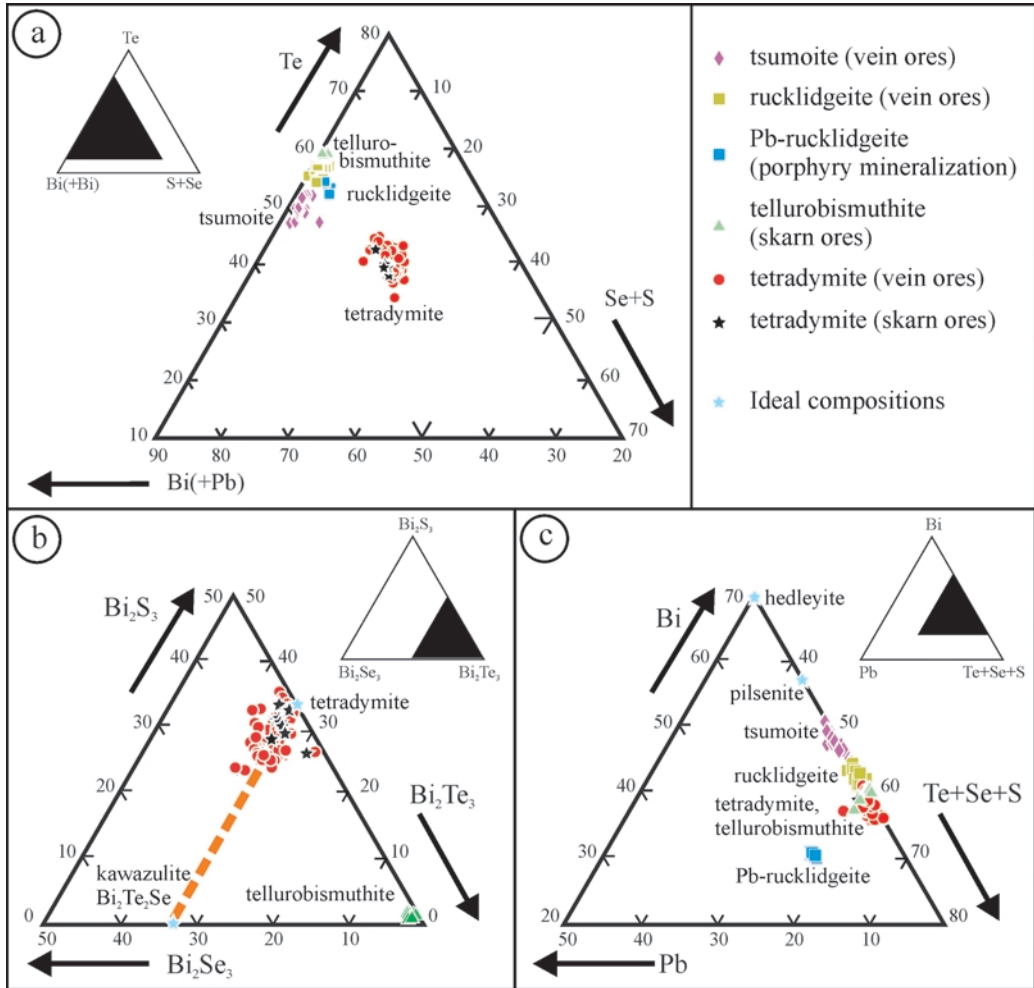* formula calculation excludes minor Ag, Cu and Fe

FIG. 6. (a) Composition of Bi-tellurides/tellurosulphides from Larga (tetradymite, tsumoite, tellurobismuthite, rucklidgeite), plotted in terms of Bi(+Pb)−Te−(S+Se). (b) Composition of tellurides and tellurosulphides in the Bi_2Te_3-Bi_2Se_3-Bi_2S_3 system demonstrating the extent of solid solution along the Bi_2Te_2S-Bi_2Te_2Se join between tetradymite, Bi_2Te_2S and kawazulite, ideally Bi_2Te_2Se. (c) Compositional variation expressed in terms of Bi-Pb-(S+Se+Te), demonstrating compositions of Pb-free rucklidgeite (vein ores) and rucklidgeite (porphyry mineralization).

level (+516 m), where they occur as elongate, <100 μm diameter inclusions within chalcopyrite, pyrite and galena (Fig. 7a). Sulphosalts are not seen in the altered skarn ('geode' area) or Cloşca veins. Lillianite homologues, lillianite, gustavite, heyrovskite and treasureite (?), are the dominant species identified, with subordinate amounts of bismuthinite derivatives, commonly intergrown with, or exsolved from the lillianite homologues (Fig. 7a). Bismuthinite derivatives (aikinite, krupkaite, bismuthinite) rarely exceed 10 μm in diameter. Cosalite is a minor constituent of some assemblages. Lillianite homologues are present as intergrowths of two or more different compositions. Within the Padina skarn mineralization, lillianite homologues form larger (200−300 μm), generally monomineralic intergrowths filling cavities, together with galena, within pyrite (Fig. 7b). We note a pavonite homologue as a minor component in a single sample. The mineral occurs as inclusions in pyrite, associated with lillianite.
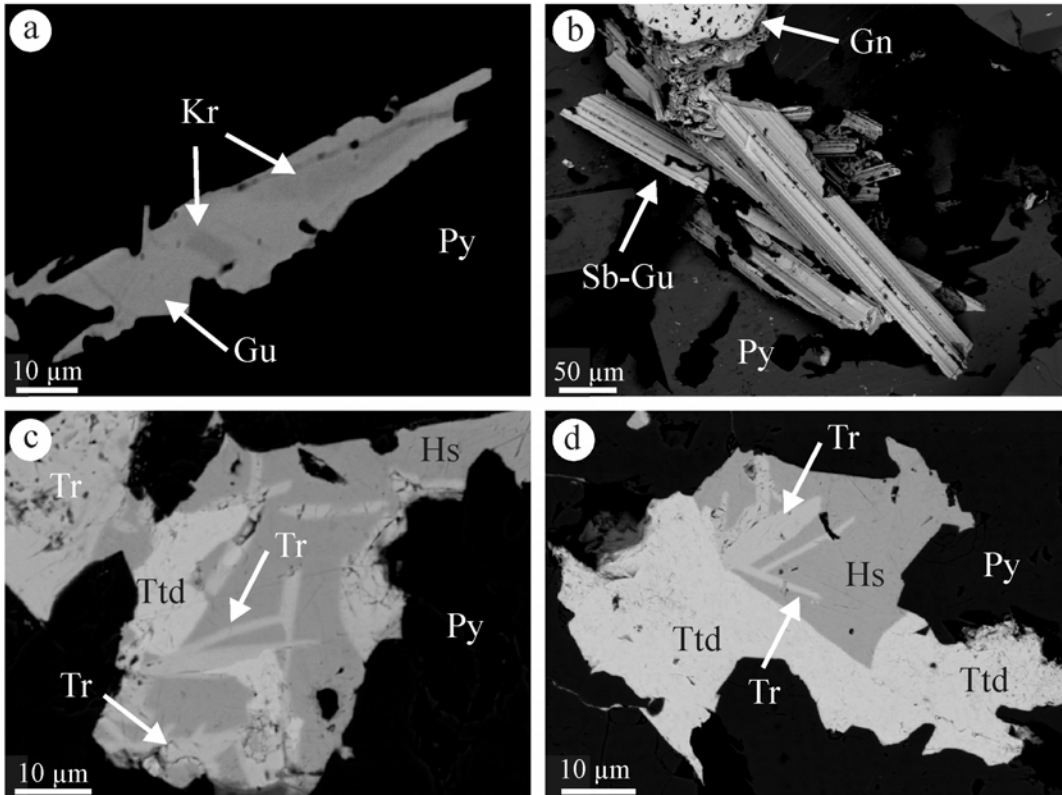
FIG. 7. BSE images showing the habit and association of Bi-sulphosalts in Larga ores. (*a*) Gustavite (Gu) as a lamellar inclusion in pyrite (Py) and containing exsolution of krupkaite (Kr). Sample: 145d (Padina vein). (*b*) Coarse crystals of Sb-gustavite (Sb-Gu), within a cavity (dark areas) on a polished specimen. Gn: galena, Py: pyrite. Sample: 145d (Padina vein). (*c*) Treasureite (Tr) as small elongate blades within hessite (Hs), intergrown with tetradymite (Ttd), enclosed within pyrite (Py). Sample: 1983/1 (Vein 37, 625 m on 0 Vest gallery). (*d*) Similar assemblage as in c. Note the apparent equilibrium boundaries between treasureite and hessite. Sample: 1983/1 (Vein 37, 625 m on 0 Vest gallery).

In the case of the vein mineralization, an intimate and apparently equilibrium assemblage of a conspicuous tabular sulphosalt (treasureite?), that occurs as masses $10-20$ μm in size, together with tetradymite and hessite is seen (Fig. 7c,d).

Composition

The [4]L lillianite homologues (lillianite and gustavite, commonly co-existing) display variable contents of both Se and Sb, ranging from virtually Se- and/or Sb-free to substituted varieties with Se/(Se+S) up to 0.22 and Sb/(Sb+Bi) up to 0.34, respectively (Table 2). Sb-bearing phases occur in both vein and skarn, but are particularly abundant in the skarn ores, which are also richer in Se. Se-rich compositional varieties generally contain

little or no Sb. Unlike lillianite-gustavite, the less abundant, [7]L homologue (heyrovskýite) appears only with an Sb-rich composition in the skarn. The microanalytical data set (Fig. 8) and high-magnification SEM investigations show abundant evidence for intergrowths of [4]L and [7]L homologues at, or below the scale of the microprobe beam, and possibly extending down to the lattice scale implying order-disorder (OD), (cf. Pring *et al.*, 1999), with many analyses plotting on a diagonal line between the [4]L and [7]L compositional lines (Fig. 8).

The mineral phase coexisting with hessite and intimately associated with tetradymite is compositionally distinct and contains more Ag than in gustavite, and also does not indicate mixing of different order homologues. The mineral, which

TABLE 2. Electron probe microanalyses of lillianite homologues.

|		Cu	Ag	Fe	Pb	Bi	Sb	S	Se	Te	Total	Calculated formula (on the basis of 11 atoms p.f.u.)
						Analysis (wt.%)						
Lillianite-gustavite												
145d	a3.p1	0.05	3.04	1.64	38.71	37.43	0.67	15.12	0.93	<mdl	97.59	$(Cu_{0.01}Ag_{0.34}Fe_{0.35})_{0.70}Pb_{2.25}(Bi_{2.16}Sb_{0.07})_{2.22}(S_{5.68}Se_{0.14})_{5.82}$
	aX.p1	1.45	4.87	0.68	31.38	42.64	0.80	15.69	1.44	<mdl	98.94	$(Cu_{0.26}Ag_{0.52}Fe_{0.14})_{0.92}Pb_{1.75}(Bi_{2.36}Sb_{0.08})_{2.44}(S_{5.67}Se_{0.21})_{5.88}$
	a2.p1	0.23	6.38	0.81	28.21	44.62	0.53	15.49	1.52	<mdl	97.77	$(Cu_{0.04}Ag_{0.70}Fe_{0.17})_{0.91}Pb_{1.60}(Bi_{2.57}Sb_{0.05})_{2.57}(S_{5.69}Se_{0.23})_{5.92}$
	a6.gr1 (§)	0.21	5.32	0.03	32.69	43.73	2.64	16.28	0.84	0.29	102.02	$(Cu_{0.04}Ag_{0.56}Fe_{0.01})_{0.61}Pb_{1.80}(Bi_{2.39}Sb_{0.25})_{2.64}(S_{5.80}Se_{0.12}Te_{0.03})_{5.95}$
	a6.gr2 (§)	0.16	7.55	0.79	22.35	50.80	0.96	15.89	1.56	0.08	100.12	$(Cu_{0.03}Ag_{0.80}Fe_{0.16})_{0.99}Pb_{1.23}(Bi_{2.78}Sb_{0.09})_{2.87}(S_{5.67}Se_{0.23}Te_{0.01})_{5.91}$
	a7.gr1 (§)	0.78	1.75	0.07	36.79	42.99	2.42	16.29	0.54	0.23	101.85	$(Cu_{0.14}Ag_{0.19}Fe_{0.02})_{0.35}Pb_{2.06}(Bi_{2.38}Sb_{0.23})_{2.61}(S_{5.88}Se_{0.08}Te_{0.02})_{5.98}$
Se-lillianite/gustavite												
145d	a6.p1	0.17	7.84	0.27	22.68	49.79	0.79	15.54	1.70	<mdl	98.79	$(Cu_{0.03}Ag_{0.85}Fe_{0.06})_{0.94}Pb_{1.28}(Bi_{2.79}Sb_{0.08})_{2.86}(S_{5.67}Se_{0.25})_{5.92}$
880/1	a5.p1	0.12	1.17	0.22	43.37	34.96	<mdl	13.01	6.51	0.20	99.56	$(Cu_{0.02}Ag_{0.14}Fe_{0.05})_{0.21}Pb_{2.61}Bi_{2.08}(S_{5.05}Se_{1.03}Te_{0.02})_{6.10}$
	a5.p3	0.13	0.32	0.20	44.40	34.90	<mdl	11.96	7.30	1.63	100.83	$(Cu_{0.02}Ag_{0.15}Fe_{0.05})_{0.22}Pb_{2.72}Bi_{2.12}(S_{4.73}Se_{1.17}Te_{0.16})_{6.06}$
	a3.p1	0.13	1.02	0.98	43.89	35.03	<mdl	13.03	5.83	0.12	100.02	$(Cu_{0.02}Ag_{0.12}Fe_{0.22})_{0.36}Pb_{2.62}Bi_{2.07}(S_{5.02}Se_{0.91}Te_{0.01})_{5.95}$
	a3.p2	0.11	1.01	1.69	43.52	34.76	<mdl	13.09	5.55	0.14	99.86	$(Cu_{0.02}Ag_{0.12}Fe_{0.37})_{0.51}Pb_{2.58}Bi_{2.04}(S_{5.00}Se_{0.86}Te_{0.01})_{5.88}$
1983/2	a1.p1	0.10	1.21	0.24	42.34	35.81	<mdl	12.80	6.48	0.20	99.17	$(Cu_{0.02}Ag_{0.14}Fe_{0.17})_{0.33}Pb_{2.57}Bi_{2.18}(S_{5.02}Se_{1.03}Te_{0.02})_{6.07}$
	a1.p3	0.08	1.23	0.22	42.32	36.21	<mdl	12.69	6.59	0.25	99.60	$(Cu_{0.02}Ag_{0.14}Fe_{0.05})_{0.21}Pb_{2.57}Bi_{2.18}(S_{4.97}Se_{1.05}Te_{0.02})_{6.05}$
Sb-lillianite/gustavite												
145d	a7.p3	0.65	5.82	0.11	33.77	34.90	6.36	15.96	1.18	<mdl	98.75	$(Cu_{0.12}Ag_{0.62}Fe_{0.02})_{0.75}Pb_{1.87}(Bi_{1.91}Sb_{0.60})_{2.51}(S_{5.70}Se_{0.17})_{5.87}$
	a7.p2	0.82	5.86	0.10	33.71	34.30	6.26	16.13	0.85	<mdl	98.01	$(Cu_{0.15}Ag_{0.62}Fe_{0.02})_{0.79}Pb_{1.86}(Bi_{1.88}Sb_{0.59})_{2.47}(S_{5.76}Se_{0.12})_{5.88}$
	a7.p5	0.70	5.36	0.11	39.98	30.59	5.11	15.56	0.97	<mdl	98.39	$(Cu_{0.13}Ag_{0.58}Fe_{0.02})_{0.73}Pb_{2.26}(Bi_{1.71}Sb_{0.49})_{2.20}(S_{5.67}Se_{0.14})_{5.81}$
	a7.p5	0.74	6.19	0.18	31.22	35.71	7.00	16.30	0.71	<mdl	98.04	$(Cu_{0.13}Ag_{0.65}Fe_{0.04})_{0.82}Pb_{1.71}Bi_{1.94}Sb_{0.65})_{2.59}(S_{5.77}Se_{0.10})_{5.87}$
	a10.11 (§)	1.43	4.20	0.12	37.27	31.92	8.67	17.02	0.66	0.24	101.53	$(Cu_{0.25}Ag_{0.42}Fe_{0.02})_{0.69}Pb_{1.96}(Bi_{1.67}Sb_{0.78})_{2.45}(S_{5.79}Se_{0.09}Te_{0.02})_{5.90}$
Treasureite												(on the basis of 60 a.p.f.u.)
1983/1	a10.p3	0.07	12.23	0.31	20.95	44.21	2.56	16.25	0.53	1.06	98.17	$Ag_{6.97}Fe_{0.34}Pb_{6.22}(Bi_{13.10}Sb_{1.29})_{14.30}(S_{31.17}Se_{0.41}Te_{0.51})_{32.09}$
	a10.p5	<mdl	10.76	0.88	23.18	44.16	1.76	15.96	0.37	0.32	97.39	$Ag_{6.25}Fe_{0.98}Pb_{7.01}(Bi_{13.23}Sb_{0.90})_{14.13}(S_{31.18}Se_{0.29}Te_{0.16})_{31.63}$
	a10.p6	<mdl	11.83	0.28	21.82	44.15	2.48	16.37	0.48	0.79	98.21	$Ag_{6.75}Fe_{0.31}Pb_{6.49}(Bi_{13.01}Sb_{1.26})_{14.27}(S_{31.44}Se_{0.37}Te_{0.38})_{32.19}$
Sb-treasureite												
1983/1	a16a.p1	<mdl	12.89	0.71	16.90	41.89	6.68	17.45	0.56	<mdl	97.07	$Ag_{6.56}Fe_{0.70}Pb_{4.48}(Bi_{11.00}Sb_{3.01})_{14.01}(S_{29.87}Se_{0.39})_{30.26}$
	a16a.p2	<mdl	13.18	0.86	16.59	40.45	7.82	16.97	0.51	0.81	97.18	$Ag_{6.72}Fe_{0.85}Pb_{4.41}(Bi_{10.66}Sb_{3.54})_{14.19}(S_{29.13}Se_{0.36}Te_{0.35})_{29.83}$
Sb-heyrovskyite												(on the basis of 34 a.p.f.u.)
3M*	a1.p1	<mdl	6.25	0.28	50.39	24.29	4.17	15.50	0.46	<mdl	101.34	$Ag_{2.08}Fe_{0.18}Pb_{8.74}(Bi_{4.18}Sb_{1.23})_{5.41}(S_{17.38}Se_{0.21})_{17.59}$
145d	a7.gr2 (§)	1.89	8.17	0.34	35.62	35.70	3.76	15.94	0.70	0.43	102.55	$(Cu_{1.02}Ag_{2.59}Fe_{0.21})_{3.82}Pb_{5.88}(Bi_{5.84}Sb_{1.06})_{6.90}(S_{17.00}Se_{0.30}Te_{0.11})_{7.41}$

all analyses made in Bristol, except marked with § (NHM)
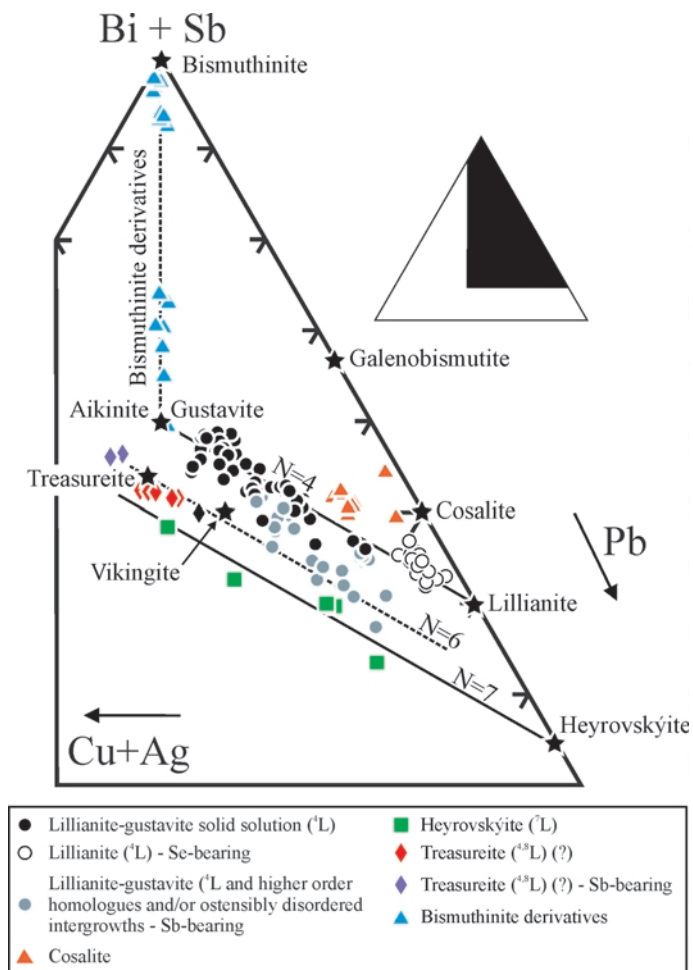
FIG. 8. Plot of compositions in (Cu+Ag)-Pb-(Bi+Sb) ternary space.

we tentatively identify as treasureite, ideally $Ag_7Pb_6Bi_{15}S_{32}$, contains more moderate concentrations of Sb and negligible Se, and conforms closely to the composition of this rare remember of the lillianite homologous series with $N_{chem} = 6$, i.e. $^{4,8}L$.

The bismuthinite derivatives aikinite (BD~94), krupkaite (BD~51) and bismuthinite (BD~9) are minor components and appear as <5 μm lamellar inclusions within lillianite. An additional sulphosalt, $Ag_{0.11}Cu_{0.02}Pb_{1.54}Bi_{2.30}S_{4.93}$, is a minor phase in the assemblage and probably represents a substituted cosalite.

Compositions of the pavonite homologue are given in Table 3. Members of this mineral group are difficult to identify on the basis of microprobe

analyses alone (e.g. Karup-Møller & Makovicky, 1979). Nevertheless, the relatively low Cu and Pb contents and tight cluster on the compositional plot in Bi-Ag-(Pb+Cu) space (Fig. 9) give us confidence to consider the mineral in question as the ^5P homologue, pavonite.

Discussion

In contrast to the abundance of Bi-sulphosalts described from deposits of the Banatitic Magmatic and Metallogenetic Belt of Romania, Serbia-Bulgaria (Ciobanu *et al.*, 2002), few have been reported previously from Neogene mineralization in Romania. The only other reported occurrences, with corroborative electron micro-

TABLE 3. Electron probe microanalyses of pavonite homologues.

Pavonite (?)	Analysis (wt.%) Cu	Ag	Fe	Pb	Bi	C	Sb	S	Se	Te	Total	Calculated formula (on the basis of 18 atoms p.f.u.)
145 13. c16 me	0.90	8.70	0.49	8.00	62.10	0.30	1.08	18.50	1.24	<mdl	101.31	$Cu_{0.25}Ag_{1.42}Fe_{0.15}Pb_{0.68}Cd_{0.05}(Bi_{5.22}Sb_{0.16})_{5.38}(S_{9.80}Se_{0.28})_{10.08}$
15. C16b	1.08	9.50	0.55	4.50	63.30	0.30	1.08	17.50	3.00	<mdl	100.81	$Cu_{0.30}Ag_{1.56}Fe_{0.18}Pb_{0.39}Cd_{0.05}(Bi_{5.37}Sb_{0.16})_{5.53}(S_{9.37}Se_{0.67})_{10.04}$
c14b 1	0.49	9.50	0.30	5.40	61.90	0.30	1.28	16.78	2.70	<mdl	98.65	$Cu_{0.14}Ag_{1.59}Fe_{0.10}Pb_{0.47}Cd_{0.05}(Bi_{5.36}Sb_{0.19})_{5.55}(S_{9.48}Se_{0.62})_{10.10}$
c16 2	1.05	8.80	0.64	7.80	61.70	0.30	1.10	18.38	1.26	<mdl	101.03	$Cu_{0.29}Ag_{1.41}Fe_{0.20}Pb_{0.65}Cd_{0.05}(Bi_{5.09}Sb_{0.16})_{5.25}(S_{9.89}Se_{0.28})_{10.17}$
c16 3	1.01	8.90	0.54	7.20	61.50	0.30	0.99	18.19	1.47	<mdl	100.10	$Cu_{0.28}Ag_{1.44}Fe_{0.17}Pb_{0.61}Cd_{0.05}(Bi_{5.12}Sb_{0.14})_{5.26}(S_{9.88}Se_{0.32})_{10.20}$
c16b 2	1.02	9.70	0.46	4.50	61.50	0.30	1.06	17.50	2.90	<mdl	98.94	$Cu_{0.29}Ag_{1.61}Fe_{0.15}Pb_{0.39}Cd_{0.05}(Bi_{5.27}Sb_{0.16})_{5.43}(S_{9.43}Se_{0.66})_{10.09}$
c16b 3	1.31	9.40	0.69	4.50	61.00	0.20	1.08	16.90	3.00	<mdl	98.08	$Cu_{0.37}Ag_{1.58}Fe_{0.23}Pb_{0.39}Cd_{0.05}(Bi_{5.30}Sb_{0.16})_{5.46}(S_{9.23}Se_{0.69})_{9.92}$
Mean ($n = 7$)	0.98	9.21	0.52	5.99	61.86	0.29	1.10	17.68	2.22		99.85	
S.D.	0.25	0.40	0.13	1.62	0.73	0.04	0.09	0.70	0.85			

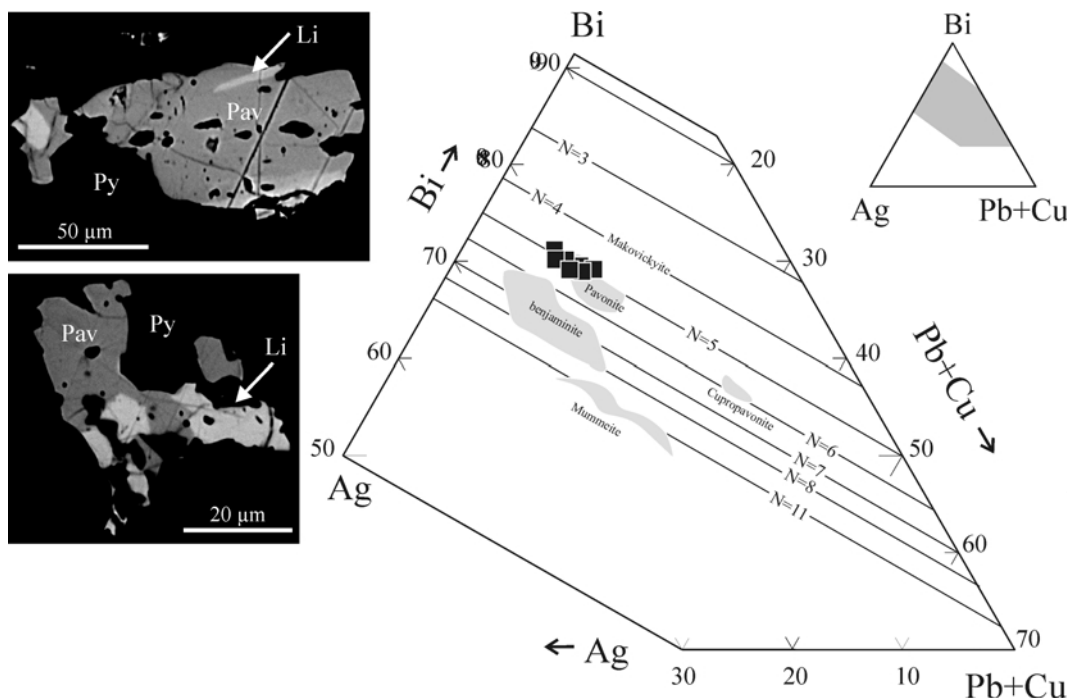all analyses made in Salzburg, Austria

FIG. 9. Compositions of pavonite homologue (^{5}P, pavonite?) plotted in Bi-Ag-(Pb+Cu) ternary space. Two back-scattered electron images show the morphology of the mineral. Pav: pavonite (?), Li: lillanite, Py: pyrite.

probe data, are within the Băiuţ-Văratec and Nistru deposits of the Baia Mare district, and the Toroiaga deposit, Baia Borşa district, in northern Romania (Cook, 1997, 1998; Damian and Cook, 1999; Damian and Costin, 1999). There are similarities between these and the Larga occurrence, both in the dominance of lillianite homologues, typical occurrence within Au-enriched pyrite (± arsenopyrite) ores, and the variable but persistent substitution of Se and Sb within the Bi-sulphosalts. This study confirms the earlier opinion that, in the Carpathian-Balkan orogens, Bi-sulphosalts are not restricted to Upper Cretaceous 'banatite' metallogenesis (e.g. Cioflica *et al.*, 1995; Cook *et al.*, 2002), but are also components of younger mineralization.

The fact that Bi-sulphosalts are more widespread than previously recognized, and the intimate relationships with Bi-tellurides/telluro-sulphides, with their distinct speciation trends, allows a number of observations to be made. Despite the fact that they occur as small or very small grains, tellurides, selenides and sulphosalts, as well as their mutual relationships, can be

valuable indicators of physicochemical conditions of formation in ore systems, because they are highly sensitive to changes in temperature, Eh-pH conditions, f_{O_2} and f_{S_2}.

Considering the dominant telluride mineralogy at different vertical levels in the hydrothermal system, Larga-Faţa Băii can be viewed as a strongly zoned system with respect to f_{Te_2}, and also to temperature. Whereas Au-tellurides and native tellurium are stable at the uppermost levels, on Horia (+516 m) level, f_{Te_2} is below the stability limit for calaverite, yet still within the stability field for tellurobismuthite and hessite. The commonly observed assemblages containing both abundant altaite and galena, sometimes sharing grain boundaries (e.g. Fig. 4c), allow a narrow domain in f_{Te_2}-f_{S_2} space to be constrained along the stability boundary between the two minerals. The absence of primary acanthite, native-Ag or -Bi allows some constraints to be made on f_{Te_2} and f_{S_2}. Applying the approach of Afifi *et al.* (1988a,b), this is interpreted to reflect an increase in $\log f_{Te_2}$ from below -10 to >-5, vertically upward from the fluid source, at $\log f_{S_2}$

of around −15 to −10 (Fig. 10). The co-existence of Bi-sulphosalts and -tellurides/tellurosulphides in the Larga veins is controlled by the parameters of the pyrite-buffered environment, close to the pyrrhotite stability field. Co-existing tellurides and tellurosulphides (tetradymite, tsumoite) have Me/Te(+Se+S) $\leqslant 1$. Such assemblages indicate relatively high f_{S_2} conditions, coupled with still relatively high f_{Te_2}. Thermodynamic data are missing for the three-component Pb-Bi-Te system, precluding correlation of telluride assemblage with f_{Te_2} and f_{S_2} to the porphyry mineralization. The presence of altaite and rucklidgeite, which also has Bi/(Te+Se+S) <1, suggests that the lowest levels of the system formed at comparable f_{Te_2} conditions as the ores of the Horia level.

The association between tetradymite and Bi-sulphosalts (e.g. aikinite-bismuthinite and lillianite series), commonly with equilibrium grain boundaries is also significant, since synthetic experiments show extensive solid solution in the Bi_2S_3-Bi_2Te_3 system, e.g. 43−66 mol.% Bi_2Te_3 at 500ºC (Yusa *et al.*, 1979). The presence of minor Pb within the 'droplets' encapsulated in pyrite, either as rucklidgeite solid solution $(Pb,Bi)_3Te_4$ or sub-microscopic blebs of galena in tetradymite, favours formation of Bi-sulphosalts and/or Bi-tellurosulphides since character-

istic order-disorder (OD) mechanisms in these minerals can be accessed to accommodate non-stoichiometry (cf. Bayliss, 1991). Both Bi-tellurosulphides and sulphosalts are commonly non-stoichiometric, a fact that can be correlated with OD in both series. If tetradymite is absent, equilibrium formation of Bi-sulphosalts is normally precluded.

Similar Bi-mineral assemblages may be expected at comparable, intermediate levels within other deposits in the region, e.g. Săcărîmb, Musariu, Măgura-Hondol), 200−400 m below those ores rich in Au-tellurides (+ native tellurium, telluroantimony etc.) at upper levels, and which contributed much of the wealth, both economic and mineralogical, for which the area is known. The occurrence of pilsenite, Bi_4Te_3, ingodite, Bi(Te,S), and aleksite, $PbBi_2Te_2S_2$, from Săcărîmb (Şimon and Alderton, 1995*a*; Shimizu *et al.*, 1999) corroborate this. Together, they may provide valuable information on the evolution of comparable complex, telluride-rich systems.

Significance for gold enrichment

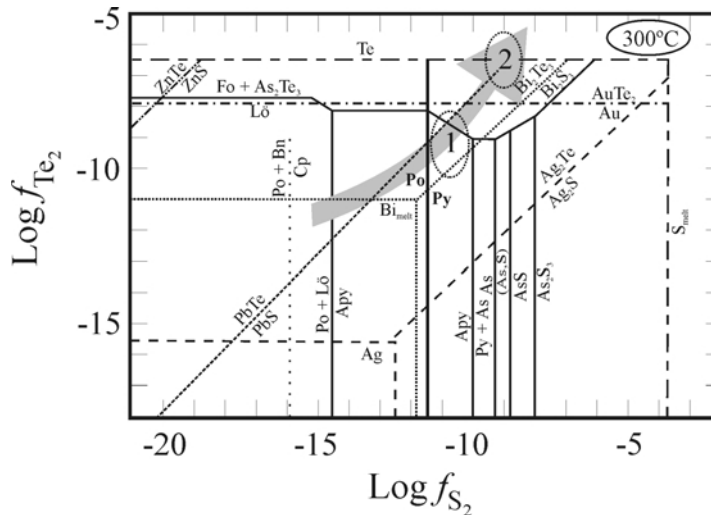Tellurides of bismuth, together with selenides and sulphosalts commonly form multi-phase eutectic/

FIG. 10. Telluride-sulphide stability diagram at 300ºC in f_{Te_2}-f_{S_2} space, after Afifi *et al.* (1988*a,b*), for mineral phases relevant to the Larga system. The grey arrow indicates the trend of mineralizing conditions from the base of the system upwards. Domains marked '1' and '2' correspond to the intermediate (i.e. Horia +516 m) and uppermost levels respectively. In the latter, Au-telluride-rich levels, calaverite and native tellurium are stable. Based on prevailing major and accessory assemblages. Abbreviations: Py: pyrite, Po: pyrrhotite, Cp: chalcopyrite, Bn: bornite, Apy: arsenopyrite, Lö: löllingite, Fo: frohbergite.

equilibrium assemblages at Larga. This feature indicates that, in many cases, extraction from mineralizing fluids closely parallels *iss* formation in the Cu-Fe-S system, in that they are extracted in the same way as Au-Bi-Te-S_{ss} droplets and crystallize in equilibrium with the host (Ciobanu and Cook, 2002). The pronounced association with gold within the 'droplets' is because it can be incorporated into Bi-melt at high aBi. Evidence for extraction of gold in droplets is seen particularly explicitly in the 'geode' ores. However, in a pyrite-buffered environment, native Bi and maldonite (Au_2Bi) are not stable. These observations are consistent with recent experiments on the partitioning of Au between hydrothermal solutions and liquid Bi showing that, above its melting point (271ºC), liquid Bi is a powerful scavenger for Au from Au-under-saturated hydrothermal solutions (Douglas *et al.* 2000).

Constraints on temperature

Although the trace mineralogy permits Larga-Faţa Băii to be viewed as a strongly zoned system with respect to the speciation of Au- and Bi-tellurides, some constraints can also be placed on temperature across the vertical extent of the Larga system. Temperatures of 400−450ºC at depth in the porphyry appear to extend, at least, to the intermediate (Horia) level at the onset of mineralization. The presence of *iss* inclusions in sphalerite from an equivalent level from Haneş (Fig. 3*f*), testify that temperatures of at least 334±17ºC (Yund and Kullerud, 1966) were attained higher up in the system. The location of the *iss* droplets within sphalerite may actually point to deposition from a $(Cu,Fe,Zn)_{1+x}S$ intermediate solid solution at temperatures as high as 500 ºC. In this line, we note that Udubaşa *et al.* (1976) used similar arguments to suggest comparable temperatures for part of the Bocşa polymetallic mineralization at Săcărîmb. More commonly, mineralization temperatures in the range 200−300ºC are commonly accepted for the area on the basis of fluid inclusion data (e.g. Borcoş, 1969; Alderton and Fallick, 2000).

Further evidence for elevated temperatures, at least in parts of the system, can be obtained from geothermometry using compositions of sphalerite-stannite pairs in the 'geode' ore (e.g. Shimizu and Shikazono, 1985). The data (Fig. 11) give temperatures between 450ºC and 350ºC, reflecting points along the cooling path at which chemical equilibrium was attained. Generally, smaller sphalerite-stannite grains (e.g. Fig. 11*a*) give temperatures closer to 350ºC, than larger grains (e.g. Fig. 11*b*), where indicated temperatures are ~450ºC. The tellurides themselves offer few temperature constraints, with the few potentially useful associations (e.g. association of tellurobis-muthite-native tellurium forming a melt eutectic at 413ºC; Elliott, 1965), not being observed in our specimens. Additional temperature constraints can be made on the presence of relict löllingite (± pyrrhotite) within arsenopyrite suggesting transition temperatures between 400 and 500ºC, given log f_{S_2} values of around −10 (Fig. 10), (Barton and Skinner, 1969).

Application to genetic model

A tectonic model for complex porphyry copper-polymetallic vein kin deposit systems, involving structural traps and tensional shear meshes within slip-fault duplexes in a supra-subduction setting have recently been applied to the Metaliferi Mts., and the Haneş-Larga field in particular (Drew *et al.*, 1999; Drew and Berger, 2001). We believe that our observations are fully concordant with such a model, in which volumes of high-temperature fluids were rapidly flushed upwards from an already emplaced porphyry system into a ready network of extensional and shear fractures. According to Drew and Berger (2001), this creates local "mesothermal"-like conditions and a ductile environment. Initial crystallization took place with pyrrhotite + löllingite as the stable assemblage. Subsequent inversion to a stable pyrite + arsenopyrite assemblage was accompanied by appearance of gold released from löllingite. This 'switch', equivalent to that diagnosed during retrograde metamorphism (Tomkins and Mavrogenes, 2001), can be considered as a sulphidation reaction, due to an increase in f_{S_2}, coupled with a decrease in f_{O_2}, drop in temperature and sudden depressurization. Simultaneously, Ag- and Bi-tellurides were extracted from fluids as Au-Bi-Te-(S) 'melts' at temperatures above the melting point of bismuth, and formed equilibrium assemblages with the bulk composition of the initial 'droplet', or alternatively, as in the 'droplets' in the 'geode' ores, decomposed during cooling (Fig. 5*d*). The speciation of Bi-tellurides, with Bi/Te(+Se+S) ⩽1 (tetradymite, tsumoite, tellurobismuthite, rucklidgeite) is consistent with a pyrite-buffered environment.
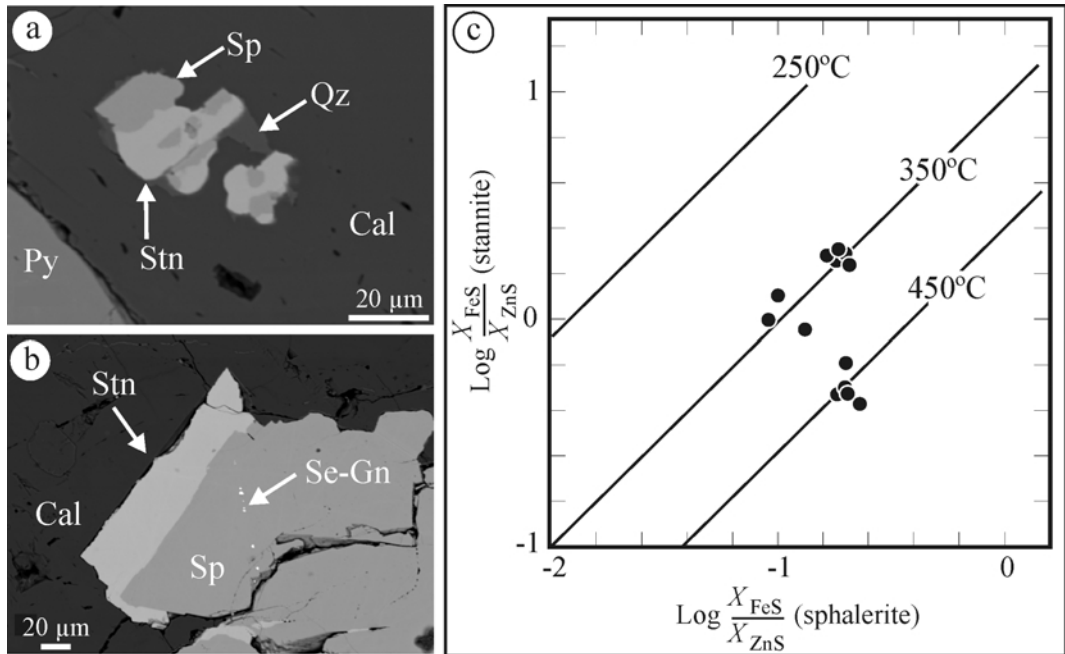
FIG. 11. Application of the geothermometric method based on the composition of coexisting stannite-sphalerite pairs in altered skarn ores from Larga. (*a*) and (*b*) BSE images showing two examples of stannite-sphalerite pairs used for geothermometry. Abbreviations: Sp: sphalerite, Stn: stannite, Qz: quartz, Cal: calcite, Se-Gn: seleniferous galena. Sample 71 (0 Est gallery). (*c*) Compositional data plotted on isotherms according to the calibration of Nakamura and Shima (1982) cited by Shimizu and Shikazono (1985). Smaller grains (e.g. *a*), give temperatures close to 350ºC.

Conclusions

(1) Sulphosalts (dominantly lillianite homologues) and tellurides/tellurosulphides of bismuth with Bi/Te(+Se+S) $\leqslant 1$ (tetradymite, tsumoite, tellurobismuthite, rucklidgeite) are significant, abundant accessories in the median part of the Larga hydrothermal system. Stable assemblages are a function of the intermediate f_{Te_2} conditions and temperatures that exceeded 400ºC.

(2) The association of sulphosalts, tellurides and gold is controlled by the pyrite-(arsenopyrite)-buffered environment, formed by sulphidation of an initial pyrrhotite-löllingite assemblage. Sulphosalts, and to some extent tellurides, are able to access changes in fluid/melt composition by order/disorder and non-stoichiometry.

(3) Tellurides are not restricted to high levels of the mineralized systems in the Metaliferi Mts. Both tellurides and sulphosalts groups help to define a zoned hydrothermal system, in which a marked f_{Te_2} decrease with depth reflects a variety of chemical environments, with Au-tellurides and native tellurium dominant at upper levels, Bi-tellurides/tellurosulphides at intermediate levels, and Bi-Pb and Pb-tellurides at depth.

Acknowledgements

References

Afifi, A.M., Kelly, W.C. and Essene, E.J. (1988*a*) Phase relations among tellurides, sulfides, and oxides: I. Thermochemical data and calculated equilibria. *Economic Geology*, **83**, 377−394.

Afifi, A.M., Kelly, W.C. and Essene, E.J. (1988*b*) Phase relations among tellurides, sulfides, and oxides: II. Applications to telluride-bearing ore deposits. *Economic Geology*, **83**, 395−404.

Alderton, D.H.M. and Fallick, A.E. (2000) The nature and genesis of gold-silver-tellurium mineralization in the Metaliferi Mountains of western Romania. *Economic Geology*, **95**, 495−515.

Barton, P.B. and Skinner, B.J. (1969) Sulfide mineral stabilities. Pp. 278−403 in: *Geochemistry of Hydrothermal Ore Deposits* (H.L. Barnes, editor). Wiley, New York.

Bayliss, P. (1991) Crystal chemistry and crystallography of some minerals in the tetradymite group. *American Mineralogist*, **76**, 257−265.

Berbeleac, I. (1986) Mineral parageneses in Tertiary gold deposits, Romania. Pp. 261−290 in: *Mineral Parageneses* (J.R. Craig, R.D. Hagni, W. Kiesl, I.M. Lange, N.V. Petrovskaya, T.N. Shadlun, G. Udubaşa and S.S. Augustithis, editors). Theophrastus Publications, Athens.

Berbeleac, I. and David, M. (1982) Native tellurium from Musariu, Brad region, Metaliferi Mountains, Romania. Pp. 283−295 in: *Ore Genesis; the State of the Art.* (G.C. Amstutz, A. El-Goresy, G. Frenzel, C. Kluth, G.H. Moh, G.H. Wauschkuhn and R.A. Zimmermann, editors). Springer, Berlin.

Berbeleac, I., Popa, T., Marian, I., Iliescu, D. and Costea, C. (1995) Neogene porphyry copper-gold, gold, and gold-bearing epithermal deposits in the South Apuseni Mountains, Romania. *Proceedings, 15th Congress, Carpathian-Balkan Geological Association*, pp. 665−670.

Borcoş, M. (1969) Le controle thermodynamique dans la métallogenèse associée au volcanisme néogène des Monts Métalliferes de la Transylvanie. *Annales de la Société Géologique de Belgique*, **92**, 307−320.

Borcoş, M. (1994) Volcanicity/metallogeny in the South Apuseni Mts. (Metaliferi Mts.). *Plate Tectonics and Metallogeny in the East Carpathians and Apuseni Mts.* Field Trip Guide, IGCP Project 356 (M. Borcoş

and Ş. Vlad, editors), Institutul Geologic al Romaniei, Bucharest, pp. 32−38.

Borcoş, M., Gheorghita, I., Bostinescu, S. and Maties, P. (1964) Considerations on some Neogene magmatic manifestations, lineaments of the Metaliferi mountains, and on the structure of the volcanic apparatus Haneş. *Dări de Seamă Comitetul Geologic*, **49**, 33−40 (in Romanian).

Borcoş, M., Kräutner, H.G., Udubaşa, G., Săndulescu, M., Năstăseanu, S., Biţoianu, C. (1983) *Mineral Resources Map of Romania, scale 1:1,000,000*, with explanatory text, 2nd edition. Institutul Geologic al Romaniei, Bucharest.

Borcoş, M., Roşu, E., Andrei, J., Bordea, S., Găbudeanu, B. and Popescu, H. (1989) *Zona Vulcanică Neogenă Zlatna-Stănija. Structural-metallogenetic map, scale 1:25,000.* Unpublished map, Institutul Geologic al Romaniei, Bucharest (in Romanian).

Ciobanu, C.L. and Cook, N.J. (2002) Tellurides, selenides (and Bi-sulphosalts) in gold deposits. *11th Quadrennial IAGOD symposium − Geocongress 2002, Windhoek, Namibia, July 2002. CD Volume of extended abstracts*. Geological Survey of Namibia.

Ciobanu, C.L., Cook, N.J. and Stein, H. (2002) Regional setting and geochronology of the Late Cretaceous Banatitic Magmatic and Metallogenic Belt. *Mineralium Deposita*, **37**, 541−567.

Cioflica, G., Jude, R., Lupulescu, M., Şimon, G. and Damian G. (1993) The tellurides of the Romanian Neogene ore deposits. Pp. 73−76 in: *Current Research in Geology Applied to Ore Deposits* (P. Fenoll Hach Ali, J. Torres-Ruiz and F. Gervilla, editors). University of Granada, Spain.

Cioflica, G., Jude, R., Lupulescu, M., Şimon, G. and Damian, G. (1995) New data on the Bi-minerals from the mineralizations related to Palaeocene magmatites in Romania. *Romanian Journal of Mineralogy*, **76**, 9−23.

Cioflica, G., Jude, R., Berbeleac, I., Lupulescu, M., Costea, D. and Costea, A. (1999) Epithermal gold mineralizations of low-sulfidation type from Baia de Arieş Mine, Southern Apuseni Mountains, Romania. *Revue Roumaine de Géologie*, **43**, 3−18.

Cook, N.J. (1997) Bismuth and bismuth-antimony sulphosalts from Neogene vein mineralisation, Baia Borşa area, Maramureş, Romania. *Mineralogical Magazine*, **61**, 387−409.

Cook, N.J. (1998) Bismuth sulphosalts from hydrothermal vein deposits of Neogene age, N.W. Romania. *Mitteilungen der Österreichischen Mineralogischen Gesellschaft*, **143**, 19−39.

Cook, N.J. and Ciobanu, C.L. (2002) Tellurides: more than mineralogical curiosities, but also markers of $fS_2 − fO_2$ evolution in zoned hydrothermal systems. *International Mineralogical Association, 18th*

General Meeting, Programme with Abstracts, Edinburgh, Scotland, p. 283.

Cook, N.J. and Ciobanu, C.L. (2003) Cervelleite, Ag_4TeS, from three localities in Romania, substitution of Cu, and the occurrence of the associated phase, Ag_2Cu_2TeS. *Neues Jahrbuch für Mineralogie, Monatshefte*, 321−336.

Cook, N.J., Ciobanu, C.L. and Bøe, R. (2001) Tellurides from the Larga hydrothermal system, South Apuseni Mountains, Romania, and their genetic significance. *Romanian Journal of Mineral Deposits*, **79** (suppl. 2), 47−48.

Cook, N.J., Ciobanu, C.L. and Bogdanov, K. (2002) Trace mineralogy of the Upper Cretaceous banatitic Magmatic and metallogenetic Belt, SE Europe. *11th Quadrennial IAGOD symposium − Geocongress 2002, Windhoek, Namibia, July 2002. CD Volume of extended abstracts*. Geological Survey of Namibia.

Damian, F. and Cook, N.J. (1999) Bi-sulphosalts from the cupriferous mineralisations from Nistru, Baia Mare area. *Romanian Journal of Mineralogy*, **79** (suppl. 1), 27.

Damian, G. and Costin, D. (1999) New data about the bismuth sulphosalts from the hydrothermal mineralisations from Văratec-Băiuţ, Baia Mare District. *Romanian Journal of Mineralogy*, **79** (suppl. 1), 28.

Douglas, N., Mavrogenes, J., Hack, A. and England, R. (2000) The liquid bismuth collector model: an alternative gold deposition mechanism. *Geological Society of Australia, AGC Abstract volume*, **59**, 135.

Drew, L.J. and Berger, B.R. (2001) model of the porphyry copper/polymetallic vein kin-deposit system: Application in the Metaliferi Mountains, Romania. Pp. 519−522 in: *Mineral Deposits at the Beginning of the 21st Century* (A. Piestrzynski *et al.*, editors). Swets and Zeitlinger Publishers, Lisse, The Netherlands.

Drew, L.J., Berger, B.R., Bawiec, W.J., Sutphin, D.M., Csirik, G., Korpás, L., Vetö-Ákos, É., Ódor, L. and Kiss, J. (1999) Mineral resource assessment of the Mátra and Börszöny-Visegrád Mountains, North Hungary. *Geologica Hungarica*, **24**, 79−96.

Effenberger, H., Paar, W.H., Topa, D., Culetto, F.J. and Giester, G. (1999) Towards the crystal structure of nagyagite, $[Pb(Pb,Sb)S_2](Au,Te)$. *American Mineralogist*, **84**, 669−676.

Elliott, R.P. (1965) *Constitution of Binary Alloys. 1st Supplement*. McGraw-Hill, New York.

Ghiţulescu, T.P. and Socolescu, M. (1941) Étude géologique et minière des Monts Metallilifères (Quadrilatère aurifère et régions environnantes). *Anuarul Institutului Geologic al Romaniei*, **21**, 181−464.

Ianovici, V., Giuşcă, D., Ghiţulescu, T.P., Borcoş, M., Lupu, M., Bleahu, M. and Savu, H. (1969) *Evolutia Geologică a Muntilor Metaliferi*. Editura Academiei Republicii Socialiste România, 741 pp. (in Romanian).

Ioan, M., Şimon, G. and Alderton, D.H.M. (1993) A new occurrence of tellurides at Magura Hondol, Metaliferi Mountains, Romania. *Romanian Journal of Mineralogy*, **76** (suppl. 1), 25.

Karup-Møller, S. and Makovicky, E. (1979) On pavonite, cupropavonite, benjaminite and oversubstituted gustavite. *Buletin de Mineralogie*, **102**, 351−367.

Kase, K., Kusachi, I. and Kishi, S. (1993) Rucklidgeite solid-solution in the Yanahara deposit, Japan. *The Canadian Mineralogist*, **31**, 99−104.

Koch, S. and Grasselly, G. (1950) Altaite from Stănija (Sztanizsa Roumania). *Acta Universitatis Szegediensis. Sectio scientiarum naturalium. (Pars Mineralogica-Petrographica)*, **4**, 47−49 (in Hungarian).

Lupulescu, M. (1997) Nagyagite: New data and considerations. *Revue Roumaine de Géologie*, **41**, 29−36.

Popescu, G.C. and Constantinescu, E. (1992) First occurrence of coloradoite in Romania. *Revue Roumaine de Géologie*, **36**, 33−34.

Popescu, G.C. and Simon, G. (1992) New tellurides from Săcărîmb, Metaliferi Mountains. *Romanian Journal of Mineralogy*, **75** (suppl. 1), 37−38.

Popescu, G.C. and Şimon, G.G. (1995) Contributions to the study of tellurides from Săcărîmb (Nagyag), Romania. *Romanian Journal of Mineralogy*, **76**, 37−42.

Pring, A., Jercher, M. and Makovicky, E. (1999) Disorder and compositional variation in the lillianite homologous series. *Mineralogical Magazine*, **63**, 917−926.

Ramdohr, P. and Udubaşa, G. (1973) Frohbergit Vorkommen in den Golderzlagerstätten von Săcărîmb und Faţa Băii (Rumänien). *Mineralium Deposita*, **8**, 179−182.

Roşu, E. (2001) Neogene magmatism in the Apuseni Mountains, Romania. Evolution and geochemical features. *Romanian Journal of Mineral Deposits*, **79** (suppl. 2), 19−22.

Shimizu, M. and Shikazono, N. (1985) Iron and zinc partitioning between coexisting stannite and sphalerite: a possible indicator of temperature and sulfur fugacity. *Mineralium Deposita*, **20**, 314−320.

Shimizu, M., Shimizu, M., Cioflica, G., Shimazaki, H., Kovacs, M., Lupulescu, M., Petrusan, G.S., Feigel, M., Popa, G., Refec, I., Pânzan, I. (1999) New informations on opaque minerals from Neogene ore deposits in Romania. *International Symposium 'Mineralogy in the System of Earth Sciences', Abstract volume*, University of Bucharest, p. 101.

Şimon, S.G. and Alderton, D.H.M. (1995*a*) Pilsenite, Bi_4Te_3 from the Săcărâmb gold-telluride deposit,

Metaliferi Mts; first occurrence in Romania. *Romanian Journal of Mineralogy*, **76**, 111−113.

Şimon, G. and Alderton, D.H.M. (1995*b*) Preliminary data for a (Au,Ag)TeO$_2$ phase from Săcărîmb gold-telluride deposit; a new mineral species or a mixture? *Romanian Journal of Mineralogy*, **77** (suppl. 1), 45.

Şimon, G., Alderton, D.H.M. and Bleser, T. (1994) Arsenian nagyagite from Sacarimb, Romania; a possible new mineral species. *Mineralogical Magazine*, **58**, 473−478.

Şimon, G., Alderton, D.H.M., Stumpfl, E.F. and Bleser, T. (1995) Tellurantimony in Romania; first occurrences in Europe. *Mineralogy and Petrology*, **53**, 115−124.

Stanley, C.J., Roberts, A.C. and Harris, D.C. (1994) New data for nagyagite. *Mineralogical Magazine*, **58**, 479−482.

Tomkins, A.G., and Mavrogenes, J.A. (2001) Redistribution of gold within arsenopyrite and löllingite during pro- and retrograde metamorphism: Application to timing of mineralization. *Economic Geology*, **96**, 525−534.

Udubaşa, G., Istate, G., Dafin, E. and Braun, A. (1976) Mineralizaţiile polimetalice de la Bocşa (N de Săcărîmb, Munţii Metaliferi). *Dari de seama ale şedinţelor, sect. 2 (Zăcăminte)*, **62**, 97−124 (in Romanian).

Yund, R.A. and Kullerud, G. (1966) Thermal stability of assemblages in the Cu-Fe-S system. *Journal of Petrology*, **7**, 454−488.

Yusa, K., Kitakaze, A. and Sugaki, A. (1979) Synthesized bismuth-tellurium-sulfur system minerals. *Science Reports of the Tohoku University, 3rd series*, **14**, 121−33.